Synergies of reducing greenhouse gases and atmospheric nitrogen pollutants in China

Xin Xu,[1,2,3,9] Xiuming Zhang,[4,9] Shaohui Zhang,[4] Wilfried Winiwarter,[4,5] Jiayu Xu,[6] Lin Zhang,[6] Chen Wang,[1,2,3] and Baojing Gu[1,2,7,8,*]
*Correspondence: bjgu@zju.edu.cn

Received: October 10, 2025; Accepted: May 20, 2026; https://doi.org/10.1016/j.xinn.2026.101433

GRAPHICAL ABSTRACT

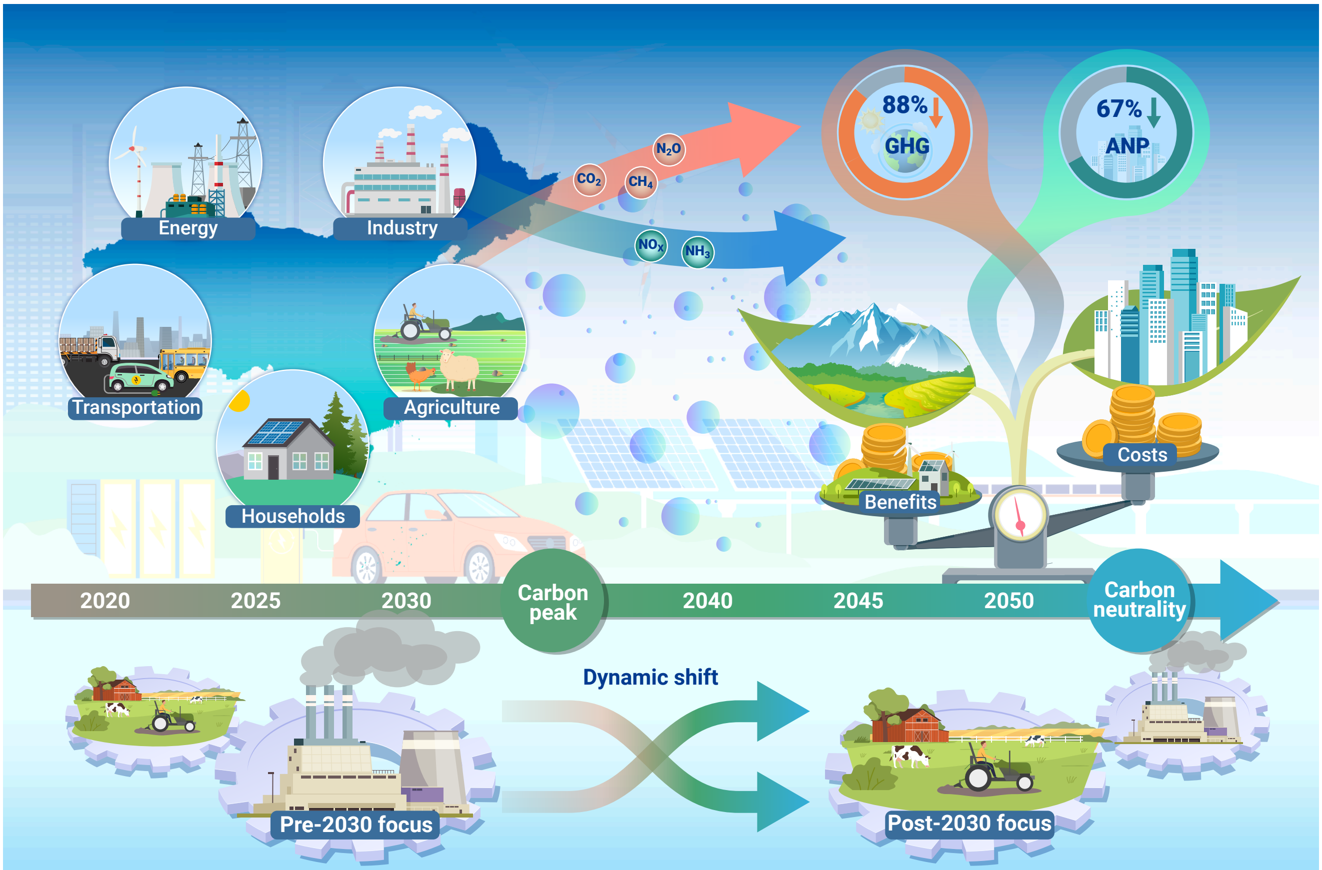

PUBLIC SUMMARY

- An integrated framework is built to quantify synergies of reducing greenhouse gases and nitrogen pollutants.
- Tiered co-control solutions and marginal abatement cost curves are proposed for synergistic management.
- Agriculture shows higher mitigation potential and cost-effectiveness than industry during deep decarbonization.

OPEN ACCESS

Geoscience ARTICLE

The Innovation

Synergies of reducing greenhouse gases and atmospheric nitrogen pollutants in China

Xin Xu,[1,2,3,9] Xiuming Zhang,[4,9] Shaohui Zhang,[4] Wilfried Winiwarter,[4,5] Jiayu Xu,[6] Lin Zhang,[6] Chen Wang,[1,2,3] and Baojing Gu[1,2,7,8,*]

[1]State Key Laboratory of Soil Pollution Control and Safety, Zhejiang University, Hangzhou 310058, China

[2]College of Environmental and Resource Sciences, Zhejiang University, Hangzhou 310058, China

[3]Policy Simulation Laboratory, Zhejiang University, Hangzhou 310058, China

[4]International Institute for Applied Systems Analysis, Laxenburg, Vienna 2361, Austria

[5]Institute of Environmental Engineering, University of Zielona Góra, 65-417 Zielona Góra, Poland

[6]Laboratory for Climate and Ocean-Atmosphere Studies, Department of Atmospheric and Oceanic Sciences, School of Physics, Peking University, Beijing 100871, China

[7]Zhejiang Provincial Key Laboratory of Agricultural Resources and Environment, Zhejiang University, Hangzhou 310058, China

[8]Ministry of Education Key Laboratory of Environment Remediation and Ecological Health, Zhejiang University, Hangzhou 310058, China

[9]These authors contributed equally

*Correspondence: bjgu@zju.edu.cn

Received: October 10, 2025; Accepted: May 20, 2026; https://doi.org/10.1016/j.xinn.2026.101433

Citation: Xu X., Zhang X., Zhang S., et al., (2026). Synergies of reducing greenhouse gases and atmospheric nitrogen pollutants in China. The Innovation **7(12)**, 101433.

Climate change and environmental degradation driven by greenhouse gases (GHGs) and reactive nitrogen (N_r) emissions are intensifying globally. As a major emitter of both, China faces double pressures of GHGs and N_r mitigation to achieve carbon neutrality and sustainability. Here, we employ a multi-model framework to quantify the potential and synergies of reducing GHG (CO_2, CH_4, and N_2O) and atmospheric N_r pollutants (NO_x and NH_3). Our results indicate that, by 2050, a strong co-control solution could reduce China's GHG emissions by 88% (80%–101%) and atmospheric N_r pollutants by 67% (50%–80%), delivering societal benefits of US$959 (US$499–US$1,419) billion, five times the implementation costs. Meanwhile, the agriculture sector will emerge as a key contributor to mitigation efforts, particularly after 2030, with its integrated abatement potential surpassing that of industry while offering superior cost-effectiveness. These findings underscore the critical need to dynamically shift mitigation priorities post-carbon peak to boost zero carbon and clean air in China.

INTRODUCTION

Excess emissions of greenhouse gases (GHGs) and reactive nitrogen (N_r) have led to various environmental threats, including climate change, air pollution, and biodiversity loss, thereby affecting ecological balance and human well-being.[1,2] China, as one of the major emitters globally,[3] has pledged to peak its carbon dioxide (CO_2) emissions before 2030 and achieve carbon neutrality before 2060, reinforcing the commitments of its nationally determined contribution under the Paris Agreement.[4] Simultaneously, China stands as a leading contributor to atmospheric nitrogen pollutants (ANPs), with the highest ammonia (NH_3) and nitrogen oxide (NO_x) emissions worldwide.[5] While substantial efforts have been made to reduce air pollutants in China through initiatives such as the Action Plan on the Prevention and Control of Air Pollution (the Clean Air Action),[6,7] persistent challenges remain, particularly in mitigating particulate matter ($PM_{2.5}$) pollution to meet the safe air quality guidelines of the World Health Organization (WHO). Moreover, despite notable declines in NO_x emissions over the past decade, mitigation for NH_3 has only recently entered the national policy agenda, as reflected in the 2023 Action Plan for Continuous Air Quality Improvement.[8]

Given the shared anthropogenic sources of GHG and ANP emissions, especially industrial and agricultural production, along with human consumption, synergistic mitigation offers the potential to concurrently alleviate the dual burdens of climate change and air pollution.[9,10] Coordinating the abatement of GHG emissions and atmospheric N_r pollution could yield multiple benefits, spreading the costs while facilitating concurrent reductions.[11,12] Optimizing technological trajectories and policy configurations to harmonize clean air initiatives with deep decarbonization targets has emerged as a focal point of scientific inquiry.[10] Previous studies have focused on the co-control potential and health co-benefits from reducing GHGs and air pollutants (especially $PM_{2.5}$), largely within the context of fossil fuel combustion and energy production.[13,14] However, research on the synergistic management of GHG and atmospheric N_r emissions remains comparatively limited and is often fragmented across specific sector or processes, such as coal combustion or rice cultivation, lacking systematic cross-sectoral comparisons.[15] As atmospheric N_r serves as a crucial precursor for $PM_{2.5}$ formation,[16] the insufficiently understood cross-sectoral mitigation mechanisms (particularly regarding NH_3) have led to an underestimation of agriculture's role in air pollution and climate adaptation.[17] Further, establishing cost-effective roadmaps for GHG and ANP co-control is imperative, but comprehensive quantifications of marginal abatement costs and their multifaceted societal benefits remain scarce.[18,19]

To bridge these knowledge gaps, this study established a multi-model assessment framework that integrates the coupled human and natural systems (CHANS) model, the GHG-air pollution interactions and synergies (GAINS) model, and the weather research and forecasting model coupled with chemistry (WRF-Chem; Notes S1–S4). Based on the CHANS simulations and an extensive literature review, we constructed comprehensive emission inventories for GHGs and ANPs in China, along with a cross-sectoral database of mitigation measures. We then projected GHG and ANP emissions from 2025 to 2050 under multiple shared socioeconomic pathways (SSPs) and co-control scenarios. Further, we quantified the mitigation potential and synergistic effects of GHG and ANP reductions across regions and sectors. Finally, we assessed the implementation costs and associated benefits of each mitigation option by examining marginal abatement cost curves (MACCs) under different scenarios. This study underscores the feasibility of synergistic mitigation strategies and offers theoretical guidance for formulating integrated dual-carbon and clean air policies in China.

MATERIALS AND METHODS

Multi-model framework

We established a multi-model framework that links the CHANS, GAINS, and WRF-Chem models through interconnected data flows and feedback loops, enabling a comprehensive analysis of emissions, mitigation costs, air quality impacts, and associated monetized estimates (Figures S1 and S2). The CHANS model quantifies GHG and ANP emission fluxes driven by human activities. The GAINS model is primarily used to assess the implementation costs and societal benefits of sector-specific mitigation technologies. The WRF-Chem model is utilized to simulate the atmospheric dispersion and chemical transformation of pollutants, providing results on air quality, regional climate impacts, and public health outcomes.

The CHANS model characterizes coupled human-natural carbon and nitrogen cycles based on national statistics and pollution surveys.[11,20] Nitrogen enters the system via biological fixation or external inputs and exits through conversion to N_2 or export, while carbon flows originate from terrestrial fixation or fossil extraction and terminate in atmospheric emissions or export. The system is disaggregated into 16 subsystems to track carbon-nitrogen flows across multiple compartments, including eight production (cropland, grassland, forest, livestock, aquaculture, industry, energy, and urban green land), three consumption (transportation, human, and pets), two post-treatment (wastewater and solid waste), and three ecology-support (atmosphere, surface water, and groundwater) subsystems.[11] The fundamental principle of the CHANS model is mass balance for both the entire system and individual subsystems (Equation 1):

$$\sum_{c=1}^{w} ACC_c = \sum_{a=1}^{u} IN_a - \sum_{b=1}^{v} OUT_b, \quad \text{(Equation 1)}$$

where IN_a and OUT_b are carbon or nitrogen inputs and outputs, respectively, and ACC_c refers to accumulation. This approach explicitly represents cascading nitrogen transformations and carbon material cycles across sectors to ensure consistency and accuracy. In this study, sectoral mappings follow the CHANS structure: the energy sector corresponds to the energy subsystem; industry to the industry subsystem; transportation sector to the transportation subsystem; households sector to the human, solid waste treatment, and wastewater treatment subsystems; and agriculture sector to the forest, grassland, cropland, and livestock subsystems (Table S1; Figure S1).

For future projection, socioeconomic drivers consistent with SSP1, SSP2, and SSP5 were incorporated exogenously into the CHANS model. Provincial energy demand forecasts are referenced from Model for Energy Supply Strategy Alternatives and their General Environmental Impact (MESSAGEix), an integrated assessment model based on the International Institute for Applied Systems Analysis (IIASA) open-source MESSAGEix-China framework, while population, economic, and land use trajectories are derived from SSP-based China datasets. The activity data (e.g., residential population, energy consumption, industrial production, agricultural output, and vehicle ownership) and emission inventories obtained from the CHANS model were transferred to GAINS for cost estimation and to WRF-Chem for air-quality simulation (Figure S2). For air quality simulation in the baseline year (2020), gridded NH_3 emissions are derived from the CHANS model,[21] while spatial grid data for other precursors, such as NO_x and SO_2, are sourced from the Multi-resolution Emission Inventory for China (MEIC) database.[22] Additional model and dataset details are provided in Note S3.

Emission inventory based on the CHANS model

GHG and ANP emission inventories were constructed based on the CHANS model, which incorporates internally consistent datasets on social-economic activity level, carbon and nitrogen process parameters, and the emission factors in China.[11] Activity data were compiled from official statistical yearbooks (Table S2), and emission factors were synthesized from peer-reviewed literature. For agriculture, the CHANS model integrated extensive data from the second national agricultural pollution census, along with over seven million farm management surveys, supporting both inventory generation and spatial analysis (Figure S3).[23] Emissions of ANPs (NH_3 and NO_x) and GHGs (N_2O, CH_4, and CO_2) were calculated as follows:

$$E_k = \sum_i \sum_k EF_{i,k} \times A_{i,k} \times \left(1 - T_{i,j,k} \times \eta_{i,j,k}\right), \qquad \text{(Equation 2)}$$

where E_k denotes the actual emission of the gas k; $EF_{i,k}$ represents the original emission factor of the source type i; and $A_{i,k}$ represents the corresponding activity level. $T_{i,j,k}$ denotes the implementation rate of the abatement option j, determined by local natural conditions, economic level, environmental objectives, and other constraints; and $\eta_{i,j,k}$ refers to the abatement efficacy.

To avoid double counting and ensure robust estimation of multi-pollutant mitigation effects, we adopted a sequential calculation framework within the integrated CHANS-GAINS model. As formalized in Equation 2, mitigation measures are applied in a fixed order to progressively adjust activity data (AD) and emission factors (EFs). First, structural and demand-side measures (e.g., industrial restructuring and dietary shifts) modify core socioeconomic drivers, thereby establishing an adjusted baseline of activity levels. Second, efficiency-enhancing measures (e.g., elevated fuel combustion efficiency and optimized fertilizer stewardship) are applied to this baseline, reducing the energy or resource intensity per unit of output. Third, end-of-pipe control technologies (e.g., filters and scrubbers) are applied to residual emissions that persist after all upstream structural and efficiency measures have been implemented. For measures operating on discrete emission sources, the aggregate mitigation potential is calculated via additive summation (Equation 3). For concurrent measures deployed within interacting systems, integrated abatement efficiencies are quantified using scenario-based functional forms (Equations 4 and 5). This parameterization isolates the net effect of each intervention, ensuring mass balance and preventing the overestimation of emission reductions across overlapping measures.[24,25]

$$\Delta E_k = \sum_i \sum_k \left(EF_{i,k} \times A_{i,k} \times T_{i,j,k} \times \eta_{i,j,k}\right) \qquad \text{(Equation 3)}$$

$$\eta_{A+B} = \eta_A + (1 - \eta_A)\eta_B \qquad \text{(Equation 4)}$$

$$\eta_{A+B+C} = \eta_A + (1 - \eta_A)\eta_B + [1 - (\eta_A + (1 - \eta_A)\eta_B)]\eta_C, \qquad \text{(Equation 5)}$$

where ΔE_k denotes the actual emission and emission reduction of the gas k. A, B, and C are the different mitigation measures included in each combination, and $\eta_{A,B,C}$ represent their corresponding abatement efficiencies.

GHG-ANP coupling index

To effectively measure the synergy of GHG and ANP emissions and reductions, we developed the GHG-ANP pollution equivalence (GNP_{eq}) indicator as a numerical scale. By assigning appropriate weights to various pollutants according to environmental regulations or their societal value, these pollutants are transformed into a single virtual pollutant (Equations 6, 7, 8, and 9):

$$E'_{NH_3} = \alpha \cdot E_{NH_3} \qquad \text{(Equation 6)}$$

$$E'_{NO_x} = \beta \cdot E_{NO_x} \qquad \text{(Equation 7)}$$

$$E'_{GHG} = \gamma \cdot E_{CO_2} + \delta \cdot E_{CH_4} + \varepsilon \cdot E_{N_2O} \qquad \text{(Equation 8)}$$

$$GNP_{eq} = W_{NH_3} \cdot E'_{NH_3} + W_{NO_x} \cdot E'_{NO_x} + W_{GHG} \cdot E'_{GHG}, \qquad \text{(Equation 9)}$$

where E_{NH_3}, E_{NO_x}, E_{CO_2}, E_{CH_4}, and E_{N_2O} indicate the actual emissions, respectively. E'_{NH_3} and E'_{NO_x} represent the nitrogen taxable equivalent in ANP_{eq}; α and β are the equivalent coefficients of NH_3 and NO_x, which are derived from the official environment tax policy in China. E'_{GHG} represents the normalized equivalent of GHGs in CO_2 equivalent (CO_{2eq}); γ, δ, and ε are the equivalent coefficients of CO_2, CH_4, and N_2O, respectively, following the global warming potential (GWP) over 100 years (1 for CO_2, 28 for CH_4, and 273 for N_2O). W_{NO_x}, W_{NH_3}, and W_{GHG} are the relative weights of NO_x, NH_3, and GHG, respectively. The conversion factors should reflect their external effects and be determined according to the influence of pollutants on living organisms and human health,[26] and we quantified the regional damage costs under different tax intensities as a suggested value for monetization (Note S1; Table S3).

Scenario design and simulation

To assess the mitigation potential of GHG and ANP synergistic management, we designed two sets of scenario pathways: baseline scenarios and co-control-based scenarios (CCBSs). Each set comprises three sub-scenarios corresponding to different SSPs and climate policy ambitions (Table S4). The SSPs provide internally consistent narratives of future trajectories in consumption patterns, technological development, and environmental awareness and are widely used for scenario-based assessments. We adopted SSP1, SSP2, and SSP5 as socio-economic baselines, representing sustainable, middle-of-the-road, and fossil fuel-intensive development pathways, respectively (Table S5). The baseline scenarios assume no additional action to address GHG or ANP mitigation challenges. Under each SSP, projected AD were incorporated into the CHANS model, propagating through changes in dietary demand, energy use, and agricultural practices to estimate GHG and ANP emissions (Table S6).

The CCBS pathways represent synergistic mitigation scenarios that simultaneously target GHG and ANP emissions under consistent levels of climate and environmental ambition. For each SSP baseline, we defined a corresponding CCBS pathways (CCBS-high, CCBS-middle, and CCBS-low), representing increasing management intensities tailored to their respective socioeconomic contexts. Future GHG mitigation stringency is guided by representative concentration pathways (RCPs), with RCP2.6, RCP4.5, and RCP8.5, paired with high, medium, and low nitrogen management intensities, while maintaining consistency with the underlying SSP assumptions. CCBS-high depicts an optimistic, sustainability-oriented future, characterized by green production and consumption, rapid deployment of high-efficiency technologies, and stringent synergistic governance. CCBS-middle a continuation of historical trends with moderate technological progress and environmental effort. In contrast, CCBS-low represents a pessimistic, fossil fuel-intensive pathway where mitigation is largely limited to incremental end-of-pipe controls with minimal structural transformation in energy and food systems (Table S4).

By integrating co-control measures and projected parameters (e.g., energy mix, diet structure, and land use change) from multiple exogenous models (Figures S4 and S5; Table S7), we executed the CHANS model to simulate emissions under each CCBS pathway. Projections were conducted at 5-year intervals from 2025 to 2050, with 2020 as the base year. To isolate the net effect of co-control interventions, the mitigation potential was calculated as the difference between each CCBS pathway and its corresponding SSP baseline (i.e., CCBS-high vs. SSP1, CCBS-middle vs. SSP2, and CCBS-low vs. SSP5). Accordingly, the gap between each baseline trajectory (dashed lines in Figure 1) and its paired CCBS pathway (solid lines in Figure 1) quantifies the net emission reduction attributable to the additional technology and policy packages. Details on projection methods and parameter settings can be found in Note S3.

To identify feasible co-control measures for China, we developed a technology-based package of mitigation measures based on previous research and a literature review, focusing on five key sectors (agriculture, energy, industry, transportation, and households; Note S2). The literature review targeted peer-reviewed publications from Web of Science

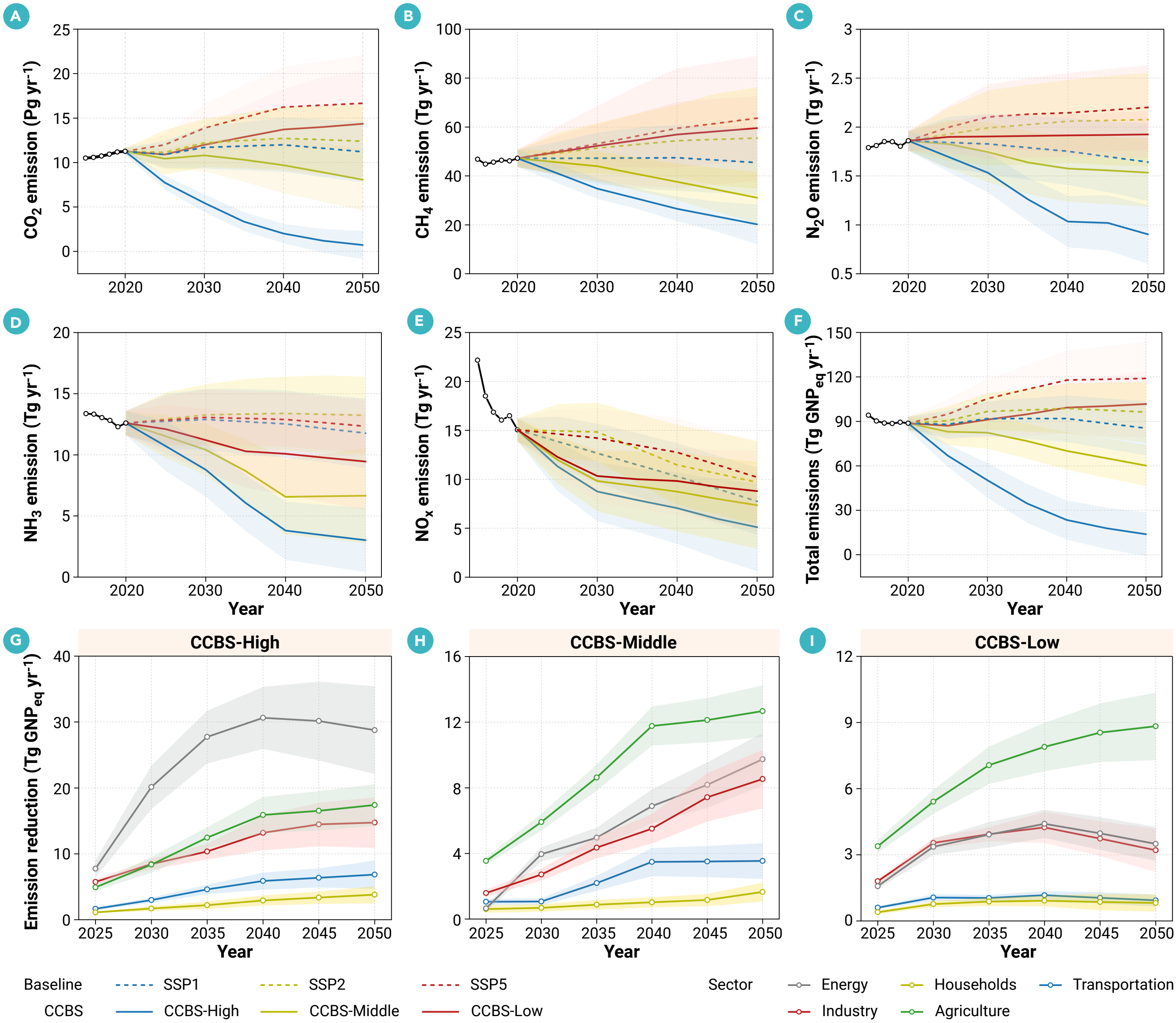

Figure 1. Emission trends of GHGs and ANPs toward 2050 under different scenarios (A) CO_2 emission (Pg CO_2 year^{-1}). (B) CH_4 emission (Tg CH_4 year^{-1}). (C) N_2O emission (Tg N_2O year^{-1}). (D) NH_3 emission (Tg NH_3 year^{-1}). (E and F) NO_x emission (Tg NO_x year^{-1}) (E) and total emissions (Tg GNP_{eq} yr^{-1}) (F) under different scenarios. The dashed lines (baseline SSP1, SSP2, and SSP5) represent the emissions driven solely by socio-economic factors without additional co-control interventions. The solid lines (CCBS-high, -middle, and -low) represent the outcomes after applying the technology and policy packages. (G–I) Sectoral GHG-ANP reductions under (G) CCBS-high, (H) CCBS-middle, and (I) CCBS-low from 2025 to 2050. The shadow behind each line shows the uncertainty range of estimation at a 95% confidence interval via 10,000 times Monto Carlo simulation (materials and methods).

since 2000. Keywords included, but were not limited to, "N_r or air pollutants", "carbon or GHG", "mitigation or abatement", "farmland or cropland", "energy or industry", "transportation or traffic", and "residential or households". Based on the identified measures, we further selected and refined efficient co-mitigation measures. Finally, a total of 28 technical measures and structural strategies were identified, with detailed information shown in the supplemental tables.

Synergistic effect evaluation

We introduced two indicators to quantitatively evaluate the mutual co-benefits between GHG and ANP emission reductions, which have been commonly employed to evaluate the magnitude of synergistic effects. The first indicator, S_1, reflecting the synergy efficiency, is the ratio of emission change of GHG to that of ANP (Equations 10, 11, and 12).

$$S_1 = \frac{\Delta E_{GHG}}{\Delta E_{ANP}} \quad \text{(Equation 10)}$$

$$\Delta E_{ANP} = \alpha \cdot \Delta E_{NH_3} + \beta \cdot \Delta E_{NO_x} \quad \text{(Equation 11)}$$

$$\Delta E_{GHG} = \gamma \cdot \Delta E_{CO_2} + \delta \cdot \Delta E_{CH_4} + \varepsilon \cdot \Delta E_{N_2O}, \quad \text{(Equation 12)}$$

where ΔE_{GHG} represents the GHG emission reduction in Tg CO_{2eq}, and ΔE_{ANP} represents the emission reduction of ANP in Gg ANP_{eq}. Higher S_1 indicates a greater reduction potential of GHGs while reducing per unit of ANP emissions simultaneously, and the closer the value is to 1, the higher the degree of synergistic reduction between them.

Further, another indicator, S_2, reflecting the coupling degree, is employed to analyze differences in the degree of coupling between GHG and ANP control in different regions or sectors.[27] The calculation is performed according to Equation 13:

$$S_2 = \frac{2\sqrt{U_{ANP} \cdot U_{GHG}}}{U_{ANP} + U_{GHG}}, \quad \text{(Equation 13)}$$

where U_{ANP} and U_{GHG} denote the provincial or sectoral abatement level for ANPs and GHGs, respectively, expressed in terms of extreme difference standardized values. Note that S_2 lies between 0 and 1; the closer to 1, the better the coupling between the GHG and ANP control systems.

Mitigation cost estimation

In this study, the mitigation costs were defined as a direct expenditure (the sum of investment costs and operation costs) for selected abatement measures (Table S8). Annual abatement costs and the future cost evolution were estimated based primarily on data from the National Bureau of Statistics of China (NBSC) and the methodology of the cost assessment from the GAINS model.[28] The total implementation cost (TC_p) in province p is calculated according to Equations 14 and 15:

$$AC_{j,p} = I_{j,p} * \left[\frac{(1+r)^{lt_{j,p}} \times r}{(1+r)^{lt_{j,p}} - 1}\right] + FO_{j,p} + VO_{j,p} - S_{j,p} \quad \text{(Equation 14)}$$

$$TC_p = \sum_{j}^{28} AC_{j,p}, \quad \text{(Equation 15)}$$

where $AC_{j,p}$ represents the annual implementation cost for measure j, $I_{j,p}$ refers to the investment cost, r is the discount rate, $lt_{j,p}$ means the lifetime of abatement technique (10–20 years), $FO_{j,p}$ is the fixed operating cost, $VO_{j,p}$ is the variable operating costs (e.g., feed, gas, electricity, labor, and water), and $S_{j,p}$ means saving costs from reduced use of energy or materials (such as N fertilizer, water, and labor). All cost data from the literature were adjusted by the purchasing power parity (PPP) index and measured in constant US\$2020 by assuming 2% annual inflation.[24]

Marginal abatement cost (MAC) refers to the cost of reducing an additional unit of emissions, typically depicted as MACC, which allows for the ranking of technologies from least to most expensive, reflecting the cost of incremental emission reductions. Here, we estimated the MACs for various GHG and ANP components and their integrated emissions based on the abatement potential and annual implementation costs (Equation 16):

$$MAC_{j,k} = \frac{\Delta IC_j}{\Delta E_{j,k}}, \quad \text{(Equation 16)}$$

where $MAC_{j,k}$ denotes the MAC for the specific mitigation measure j and emission species k, ΔIC_j is the change in implementation cost associated with the measure j, and $\Delta E_{j,k}$ is the change in emissions due to the implementation of the measure j.

Societal benefit assessment

The societal benefits ($SOC_{benefit,y}$) of GHG and ANP co-control for year y are defined as the sum of benefits for human health ($HH_{benefit,y}$), ecosystem service ($EH_{benefit,y}$), and climate impact ($CL_{impact,y}$), as shown in Equation 17:

$$SOC_{benefit,y} = HH_{benefit,y} + EH_{benefit,y} + CL_{impact,y}. \quad \text{(Equation 17)}$$

Health benefits refer to the benefit of prevented mortality due to the alleviation of $PM_{2.5}$ pollution. First, we used the WRF-Chem model to simulate the annual $PM_{2.5}$ concentrations for the baseline year and future scenarios. Then, drawing on the global burden of disease (GBD) framework,[29] we combined the exposure-response relationships (Equation 18) with the health effect function (Equation 19) to estimate the premature mortality attributable to $PM_{2.5}$ exposure. Subsequently, we applied the updated China-specific value of statistical life (VSL) to quantify the associated economic benefits, following the methodology of Giannadaki et al.[17] (Equation 20). Note that, to isolate the health benefits resulting from ANP mitigation, this study excludes the co-benefits from the reduction of other precursors, such as non-methane volatile organic compounds (NMVOCs):

$$HE_{y,q} = \sum_{y} e^{\beta_q * (C_{co,y} - C_{base,y})} * HE_{0,q} \quad \text{(Equation 18)}$$

$$\Delta M_y = \sum_{q} (HE_{y,q} - HE_{0,q}) * POP_y \quad \text{(Equation 19)}$$

$$HH_{benefit,y} = VSL_y * \Delta M_y, \quad \text{(Equation 20)}$$

where $C_{co,y}$ and $C_{base,y}$ are the annual average $PM_{2.5}$ concentration under CCBS and baseline pathways, respectively. The subscript q represents disease categories, including interstitial lung disease (ILD), chronic obstructive pulmonary disease (COPD), ischemic heart disease (IHD), lung cancer (LC), and cerebrovascular disease (CEV). β_q is the coefficient in the exposure-response function, representing the proportion change in each health endpoint per unit change in $PM_{2.5}$ concentration. C_0 is the background concentration below which no health impact is assumed and is set at 10 $\mu g\ m^{-3}$, as suggested by the WHO. $HE_{0,q}$ is the baseline health effect due to a particular disease category for China, as estimated by the GBD. $HE_{y,q}$ is the actual health effect under prevailing $PM_{2.5}$ pollution levels. POP_y is the population exposed to air pollution in China. ΔM_y denotes the number of avoided premature deaths, and VSL_y is the VSL for China derived from Xie et al. Further information about air quality simulation can be found in Note S3. Simulated $PM_{2.5}$ concentrations and aerosol fields were evaluated against observational data from monitoring sites (Figures S6 and S7).

Ecosystem benefits ($EH_{benefit}$) are regarded as the avoided damage costs associated with reduced ecosystem acidification and eutrophication. Baseline ecosystem damage costs were derived from the European Nitrogen Assessment[30] and peer-reviewed studies (Table S9). Avoided ecosystem damage costs were then calculated using Equations 21, 22, and 23:

$$EH_{benefit,y} = \sum_{k}^{5} \left(E_{base,y,k} * Ecost_{base,y,k} - E_{co,y,k} * Ecost_{co,y,k}\right) \quad \text{(Equation 21)}$$

$$Ecost_{base,y,k} = Ecost_{2020,k} * \sqrt[\beta]{\frac{PGDP_{base,y}}{PGDP_{2020}}} * \frac{Density_{base,y,k}}{Density_{2020,k}} \quad \text{(Equation 22)}$$

$$Ecost_{co,y,k} = Ecost_{2020,k} * \sqrt[\beta]{\frac{PGDP_{co,y}}{PGDP_{2020}}} * \frac{Density_{co,y,k}}{Density_{2020,k}}, \quad \text{(Equation 23)}$$

where $Ecost_{2020,k}$ denotes the monetized ecosystem damage costs of gas k in 2020. $Ecost_{base,y,k}$ and $Ecost_{co,y,k}$ refer to the corresponding ecosystem damage costs in year y under the baseline and CCBS pathways, respectively. The coefficient β is an adjustment factor for ecosystem damage costs, derived from empirical relationships between historical damage costs, per capita gross domestic product (PGDP), and emission intensity.

Climate impact ($CI_{benefit}$) refers to the reduction of GHG and the alteration of the cooling effect that N_r emissions have on the Earth system. Warming effects from CO_2, CH_4, and N_2O were quantified using monetized parameters from studies on the social cost of carbon.[31] The net cooling effects of NH_3 and NO_x generally involve increased aerosol loads, shortened CH_4 lifetimes, and enhanced land carbon sequestration associated with the anthropogenic N_r increase.[32] The monetized parameters for these effects are sourced from the European Nitrogen Assessment and relevant global assessments,[32,33] with adjustments based on China-specific aerosol simulations (Equations 24, 25, and 26):

$$CI_{impact,y} = \sum_{k}^{5} \left(E_{base,y,k} * CI_{base,y,k} - E_{co,y,k} * CI_{co,y,k}\right) \quad \text{(Equation 24)}$$

$$CI_{base,y,k} = CI_{2020,k} * \sqrt[r]{\frac{PGDP_{base,y}}{PGDP_{2020}}} * \frac{Density_{base,y,k}}{Density_{2020,k}} \quad \text{(Equation 25)}$$

$$CI_{co,y,k} = CI_{2020,k} * \sqrt[r]{\frac{PGDP_{co,y}}{PGDP_{2020}}} * \frac{Density_{co,y,k}}{Density_{2020,k}}, \quad \text{(Equation 26)}$$

where $CI_{2020,k}$ refers to the monetized climate impact of gas k (CO_2, CH_4, N_2O, NH_3, and NO_x) in China for 2020. $CI_{base,y,k}$ and $CI_{co,y,k}$ refer to the regional monetized climate impacts under baseline and CCBS pathways in year y, respectively. The coefficient γ is a provincial adjustment factor derived from empirical relationships between historical damage costs, PGDP, and emission intensity.

Uncertainty analysis

The integration of a mass-balance framework provides a robust biophysical constraint on the emission inventory, minimizing cumulative error propagation by enforcing mass conservation across compartmental transfers.[34] Despite these constraints, inherent uncertainties persist due to heterogeneities in data quality and parameter applicability. In this study, uncertainty propagation was quantified using a Monte Carlo simulation approach with 10,000 iterations. Regional discrepancies in activity levels, stemming from divergent statistical protocols, reporting biases, and survey granularities, constitute the primary sources of unavoidable error. Input uncertainties were characterized using coefficients of variation (CVs), derived from an extensive literature review and expert judgment (Table S2). Parameters adopted from international studies were assigned higher CVs to reflect lower regional specificity. In addition, a semi-quantitative confidence classification was applied to AD and emission parameters, distinguishing five tiers: very high (±5%), high (±5%–33%), medium (±33%–67%), low (±67%–95%), or very low (±95%). For each iteration, input parameters were randomly sampled from their respective probability distributions (typically normal or log-normal, depending on the parameter type) to generate 95% confidence

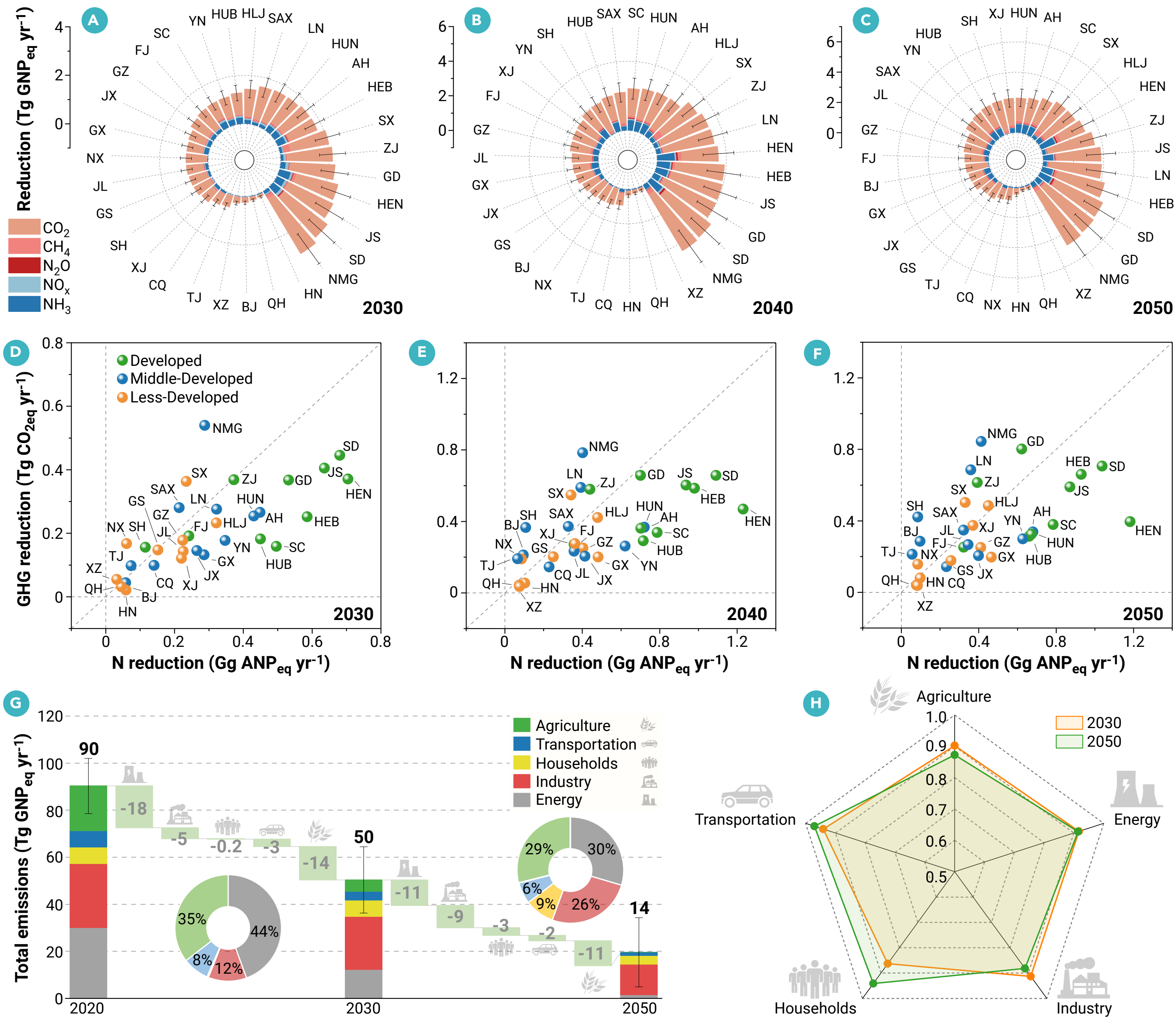

Figure 2. Synergistic mitigation across regions and sectors under the CCBS-high pathway (A–C) Provincial-scale synergistic mitigation potential in (A) 2030, (B) 2040, and (C) 2050, expressed as Tg GNP$_{eq}$ year^{-1}. The error bars represent the uncertainty ranges (95% confidence intervals) derived from 10,000 Monte Carlo simulations. (D–F) Characteristics between GHG and ANP reductions at the provincial scale under the CCBS-high pathway in (D) 2030, (E) 2040, and (F) 2050. Blue, green, and orange dots indicate developed, middle developed, and less developed provinces, respectively, classified by provincial GDP (Figure S17). Provincial abbreviations are listed Table S10. (G) Sectoral contributions to integrated GHG-ANP reduction potential in 2030 and 2050, expressed as Tg GNP$_{eq}$ year^{-1}. (H) Coupling degrees (S_2) of sectoral GHG and ANP reductions in 2030 and 2050.

intervals for both historical inventories and future projections. The internal consistency and robustness of the historical emission estimates were validated through cross-comparisons with global databases and independent peer-reviewed studies (Figure S8; Note S5).

RESULTS AND DISCUSSION

Synergistic mitigation potential

Over the past two decades, China's anthropogenic GHG and ANP emissions have exhibited partially divergent trajectories (Figure S8). Between 2000 and 2010, emissions of both GHGs and ANPs increased rapidly, driven by population growth and the expansion of fossil fuel use.[35] Thereafter, GHG emissions continued to rise, reaching 11.8 $\pm$ 0.7 petagrams (Pg) CO_2 year^{-1}, 47.4 $\pm$ 7.1 teragrams (Tg) CH_4 year^{-1}, and 1.8 $\pm$ 0.2 Tg N_2O year^{-1} by 2020 (Figure S9). In contrast, the implementation of air pollution control policies since 2013 led to a marked decline in NO_x emissions,[36] while agricultural interventions, such as the zero-growth fertilizer initiative, contributed to the reduction of NH_3 emissions after 2016.[37] Spatially, GHG and ANP emissions display broadly consistent but sector-specific patterns (Figure S10). CO_2 and NO_x emissions are concentrated in major urban and industrial regions,[38,39] whereas NH_3 and N_2O emissions are primarily associated with agricultural hotspots.[40,41] These historical trends reveal the structural drivers of emissions and underscore the tight coupling between climate and nitrogen pressures, providing an empirical backdrop for assessing future synergistic mitigation potentials.

Future emission trends and the reduction potential of GHGs and ANPs in China were simulated under two suits of scenarios: (1) three baseline SSPs (SSP1, SSP2, and SSP5), and (2) three CCBSs (CCBS-high, -middle, and -low) related to these SSPs. The worst-case baseline, SSP5, shows a substantial surge in emissions by 2050, with CO_2, N_2O, and CH_4 increasing by 48%,18%, and 35% relative to 2020, respectively (Figures 1A–1C). NH_3 emissions are expected to remain stable at 12.8 $\pm$ 0.2 Tg year^{-1}, while NO_x emissions will decrease by 32% relative to 2020 (Figures 1D and 1E). Under the better performing baselines, SSP1 and SSP2, emissions are modestly lower than under SSP5. For instance, emissions under the SSP1 pathway are 5%–30% below SSP5 levels across all species by 2050, mainly driven by enhanced environmental awareness and demand shifts.[42] However, these socioeconomic changes

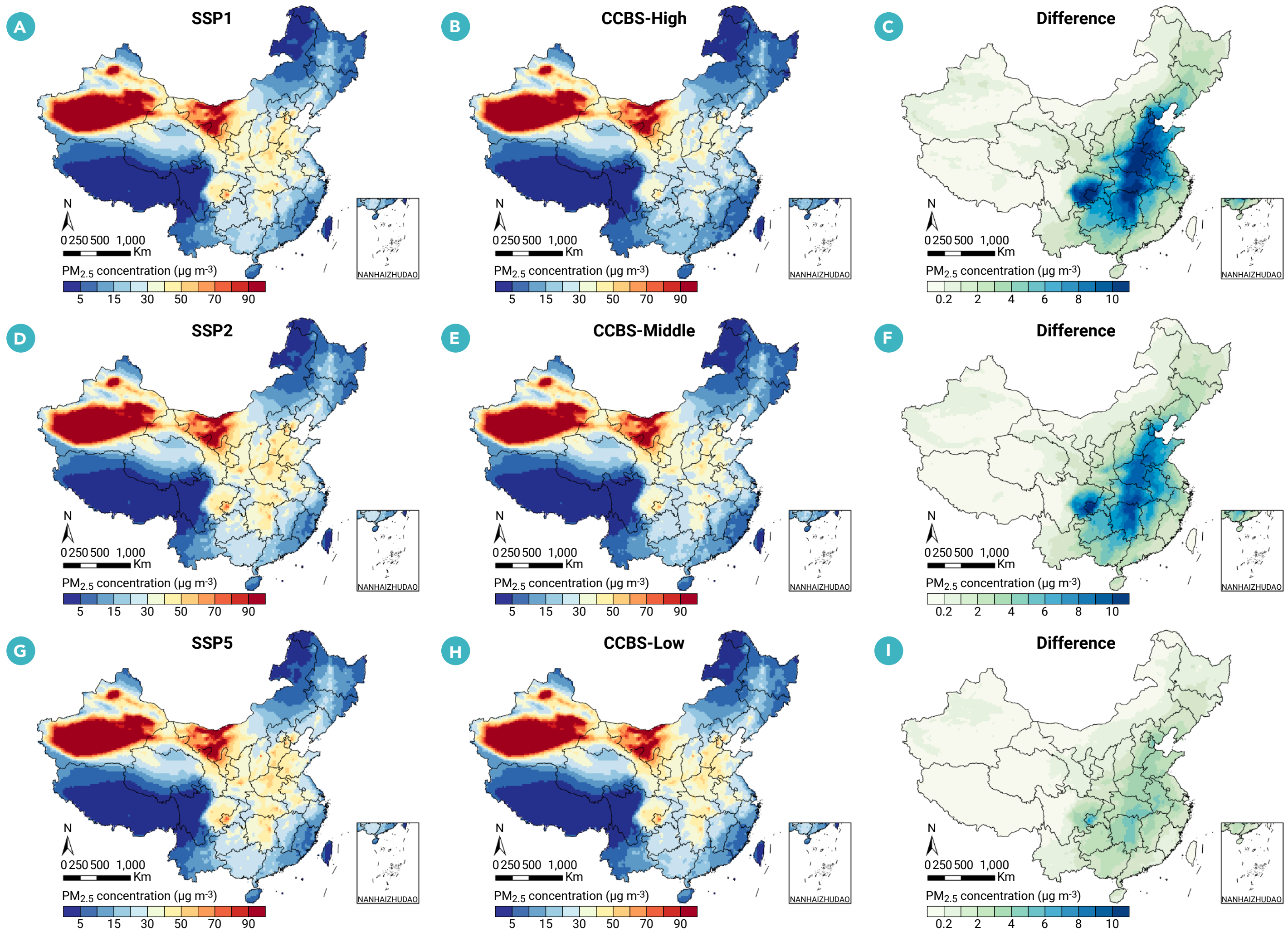

Figure 3. Atmosphere $PM_{2.5}$ concentration under different scenarios in 2050 Shown is the geographic distribution of surface air $PM_{2.5}$ concentration in 2050 under the baseline scenarios (A) SSP1, (D) SSP2, and (G) SSP5; the co-control scenarios (B) CCBS-high, (E) CCBS-middle, and (H) CCBS-low; and the corresponding differences between CCBS and baseline scenarios (C, F, and I). A comparison of baseline-year aerosol distributions with the observation-based dataset can be found in Figures S6-7.

alone are insufficient to meet ambitious mitigation targets, necessitating targeted intervention strategies. By incorporating cross-sectoral abatement measures into the CHANS model, the CCBS pathways reveal divergent emission magnitudes and trajectories. Under the SSP1-CCBS-high (CCBS-high), GHG emissions exhibit a consistent decline by 2050, with reductions of 94% for CO_2, 51% for N_2O, and 57% for CH_4, compared to 2020, respectively (Figures 1A–1C). Concurrently, NO_x and NH_3 emissions are projected to fall by 66% and 76%, respectively (Figures 1D and 1E). The SSP2-CCBS-middle pathway (CCBS-middle) also achieves emission reductions, albeit to a lesser extent, whereas SSP5-CCBS-low (CCBS-low) fails to curb CO_2 and CH_4 emissions due to sustained fossil fuel demand, with only marginal decreases in NH_3 and NO_x compared to 2020 (Figure 1).

To ensure comparability of overall mitigation potential, we developed a GNP_{eq} index, which weighs GHG and ANP emissions based on their social costs, derived from carbon pricing and pollution damage estimates[26] (Figure 1F; Table S3). In essence, this index compares pollution burdens based on legislatively defined damage attribution and serves as a policy-weighted scoring metric rather than a physical emission indicator (Note S1). Under the CCBS-high pathway, the energy sector is the dominant contributor to GHG and ANP synergistic mitigation, accounting for 43% of the total GNP_{eq} reduction, although its marginal mitigation potential declines after 2040 (Figure 1G). Industry and agriculture follow with broadly comparable contributions (Figure 1G). Remarkably, the contribution of agriculture is projected to surpass that of industry by 2030, reaching 17.4 ± 2.0 Tg GNP_{eq} $year^{-1}$ (0.9 Pg CO_2 $year^{-1}$, 7.6 Tg CH_4 $year^{-1}$, 0.6 Tg N_2O $year^{-1}$, 8.6 Tg NH_3 $year^{-1}$, and 0.4 Tg NO_x $year^{-1}$) by 2050, underscoring its considerable but often underappreciated potential of agriculture for synergistic reductions of GHG emission and nitrogen pollution. This temporal lag could be attributed to the more rapid transformation and deployment of technological solutions in China's industrial sector,[43] whereas the fragmented nature of agriculture, such as small farm size, policy complexities, and the time required to change management practices, slows the abatement pace.[44]

Under the CCBS-middle pathway, synergistic mitigation in the energy and industrial sectors increases steadily but remains moderate (Figure 1H). Conversely, agriculture emerges as the dominant contributor, contributing over 40% by 2050, with 17% to GHG reduction and 89% to ANP reduction. A similar pattern is observed under CCBS-low, where agriculture contributes, on average, 44% of total mitigation, primarily driven by nitrogen management practices and soil carbon sequestration. Contributions from the energy and industrial sectors remain limited, while the transportation and residential sectors continue to play minor roles (Figure 1I). Overall, the relative importance of agriculture is expected to increase after China's anticipated carbon peak around 2030, and the regional heterogeneity in sectoral contributions reflects divergent development pathways and resource endowments (Figures S11 and S13). These sectoral patterns are robust across alternative damage attribution frameworks under different tax levels (Figure S14).

Spatially, provinces with higher synergistic mitigation potential are mainly concentrated in the eastern and southern regions, exemplified by Jiangsu, Guangdong, and Shandong (Figures 2A–2C and S15). These provinces also rank among the national leaders in agricultural, industrial, and economic development, reflecting stronger capacity to adopt advanced technologies and implement sustainable practices (Figures S16 and S17). Along the CCBS-high

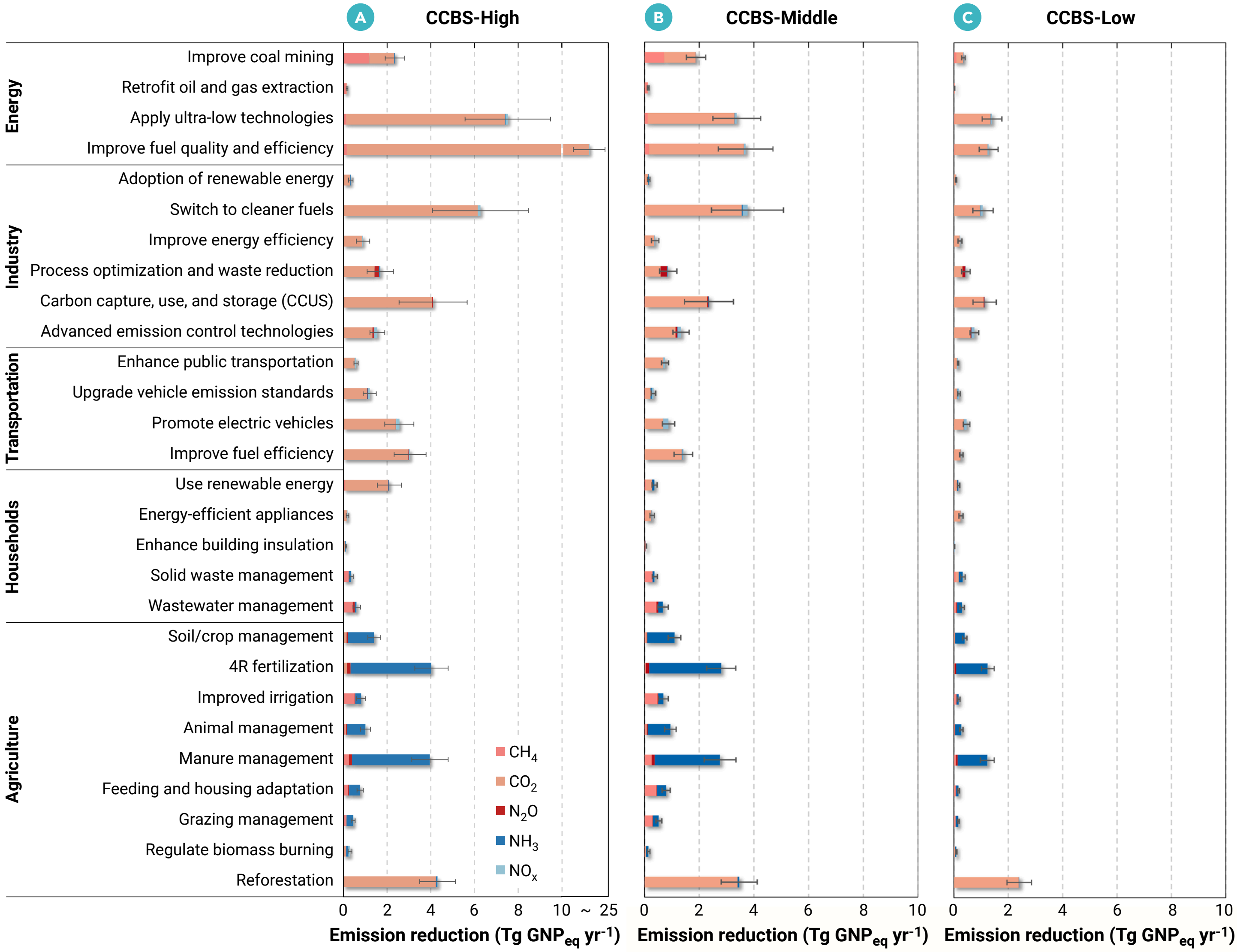

Figure 4. Sub-sectoral GHG and ANP synergistic abatement potential in 2050 Shown are the synergistic mitigation contributions of individual measures in 2050 under the (A) CCBS-high, (B) CCBS-middle, and (C) CCBS-low pathways, expressed in Tg GNP_{eq} year^{-1} (materials and methods). The error bars represent the uncertainty ranges (95% confidence intervals) associated with parameter values compiled from the literature and data sources. Detailed descriptions of the measures are provided in the supplemental tables.

pathway, most provinces are capable of synchronous GHG and ANP abatement management, although regional priorities vary with industrial structure, resource endowments, and development trajectories (Figures 2D–2F and S18). For instance, provinces with a legacy of heavy industry, including oil, mining, and manufacturing, such as Inner Mongolia and Liaoning, derive larger GHG mitigation benefits from industrial co-control measures. In contrast, Qinghai and Tibet, endowed with substantial soil carbon sequestration and renewable energy potential, may realize greater advantages by prioritizing co-control strategies that leverage these assets. Importantly, stringent co-control management is projected to lower the national average $PM_{2.5}$ concentration by 35%, from 34 μg/m^3 in 2020 to 22 μg/m^3 by 2050, with pronounced air quality improvements in Hunan, Chongqing, Hubei, and Anhui (Figure 3). These benefits reflect environmental gains attributable solely to atmospheric nitrogen pollution control. When synergies among multiple air pollutants are considered, these interventions may generate greater health co-benefits, accelerating progress toward the ambitious global air quality standards proposed by the United Nations Environment Program.[45]

Synergistic mitigation effects

To quantify the synergistic effects under different co-control solutions, we introduced two coefficients (S_1 and S_2) to assess the interplay between GHG and ANP emission reductions (materials and methods). S_1 reflects the physical synergy efficiency, while S_2 represents the coupling degree within the control systems. At the national level, the average synergy efficiency (S_1) over 2025–2060 under the CCBS-high, CCBS-middle, and CCBS-low pathways is 4.9 (4.6–5.2), 2.0 (1.5–3.0), and 2.9 (2.5–3.1), respectively, implying that reductions in ANP are associated with multiplicative reductions in GHG emissions (Figures S19 and S20). Under the CCBS-high pathway, each unit of ANP reduction is accompanied by an approximately five-unit reduction in GHG emissions, with higher synergies observed in Shanghai, Beijing, and Inner Mongolia. Notably, by 2030, the coupling degree (S_2) exceeds 0.9 across all three CCBS pathways, suggesting a high level of coordination between the embedded measure portfolio for GHG and ANP control.

At the sectoral scale, under the CCBS-high pathway, China's integrated emissions will fall by 44% by 2030 compared to 2020, with contributions from energy (44%), agriculture (35%), industry (12%), and transportation (8%). From 2030 to 2050, a further 72% reduction is expected, driven primarily by energy and agricultural sectors (Figure 2G). Notably, benefitting from carbon sequestration, agriculture will achieve negative emissions of 5.7 Tg GNP_{eq} year^{-1} (−1.6 Pg CO_2 year^{-1}, 7.5 Tg CH_4 year^{-1}, 0.6 Tg N_2O year^{-1}, 2.2 Tg NH_3 year^{-1}, and 0.6 Tg NO_x year^{-1}) by 2050. Figure 2H delineates the coupling degrees (S_2) of GHG and ANP mitigation across sectors under the CCBS-high pathway. All sectors play a distinct role, with the average S_2 exceeding 0.8. In particular, the transportation and household sectors exhibit higher S_2, reaching 0.97 and 0.94 by 2050, respectively, indicating near-synchronous reductions in GHG and ANP emissions. For the energy and industry sectors,

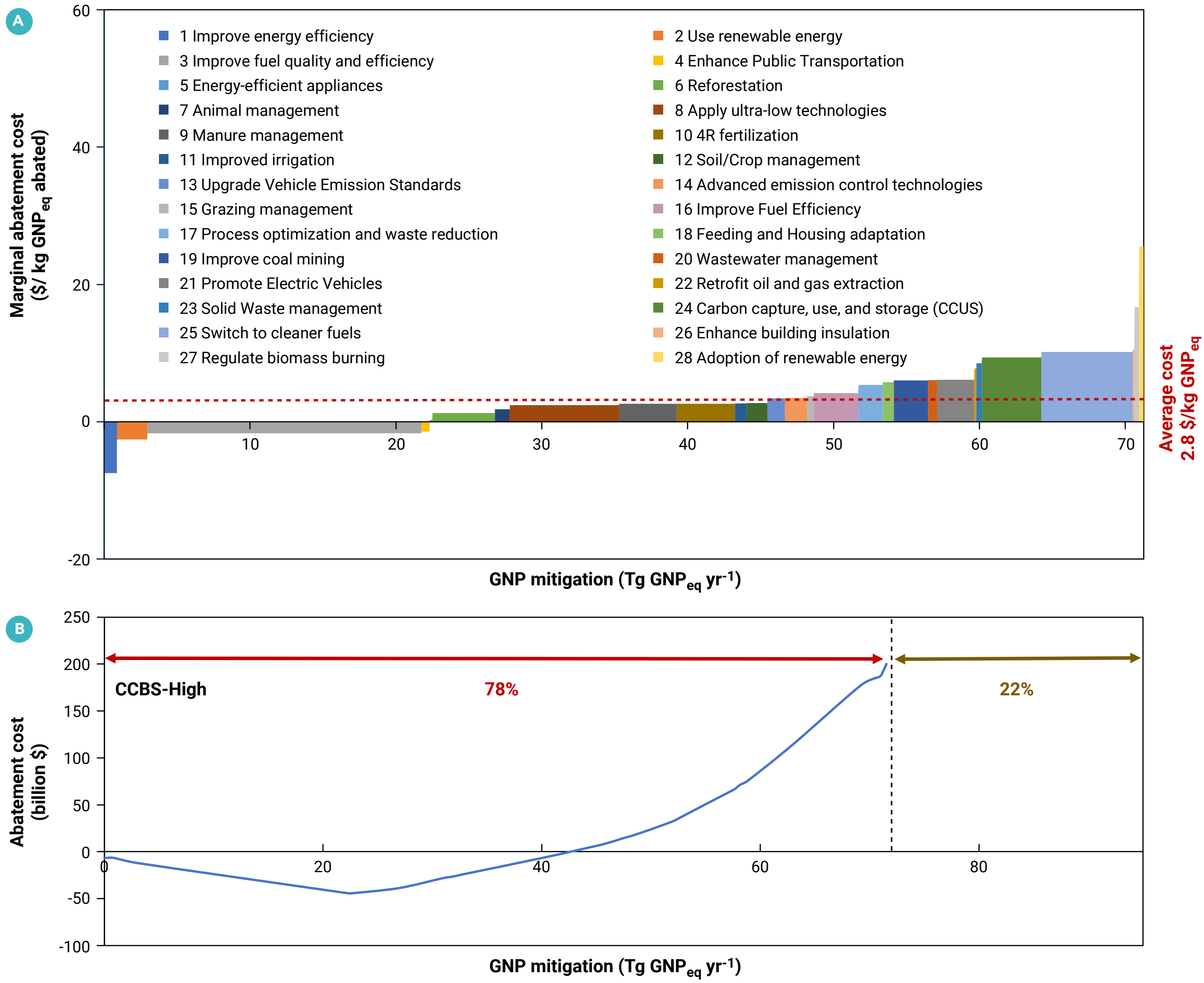

Figure 5. MAC of GHG-ANP synergistic mitigation under CCBS-high in 2050 (A) MACs of 28 co-control measures in 2050, with average cost of US\$2.8 per kg GNP_{eq} abated. The measures are ordered according to increasing MACs. (B) Cumulative abatement cost curve under CCBS-high with 78% mitigation potential compared to baseline. MACCs for CCBS-middle and CCBS-low can be found in Figures S25 and S26.

measures such as phasing out outdated capacity and promoting cleaner fuels are expected to further curb both GHG and ANP emissions, especially in Shaanxi, Shanxi, and the Northeast regions. Meanwhile, synergistic mitigation in the transportation and household sectors is mainly achieved through the adoption of clean energy and greener consumption patterns, particularly in densely populated or coal heating-dependent regions, such as East and Northeast China. Although agriculture shows lower physical synergy owing to limited CO_2 emissions, practices such as soil/crop management and enhanced carbon sinks play an indispensable role in GHG and ANP co-control, especially in major grain-producing regions such as the North China Plain and the Fenwei Plain.[46]

Under the CCBS-middle pathway, the co-control potential is modest, with a 9% reduction by 2030 and an additional 27% feasible by 2050 (Figure S21). Under the CCBS-low pathway, insufficient progress in energy transition leads to a 12% increase in integrated emissions by 2050. Encouragingly, activated carbon sequestration is expected to offset approximately 6.5% of GHG emissions, providing further evidence of the critical role of agriculture in co-controlling GHG and ANP emissions (Figure S21). These findings underscore the pivotal role of structural transformation and policy guidance in promoting cross-sectoral synergistic mitigation, particularly through targeted prioritization of measures in various regions.

Cost-benefit analysis

Embedded in the co-control solutions, we synthesized 28 mitigation measures and quantified their mitigation potentials and MACCs, uncovering the co-benefits for abating GHG and ANP emissions simultaneously (Figures 4 and 5). By 2050, the high-intensity implementation of co-control measures could reduce overall emissions by 78% compared to the SSP1 baseline, with an average MAC of US\$2.8 per kilogram (kg) of GNP_{eq} (Figure 5). The corresponding average costs are estimated at US\$13.2 per ton of CO_{2eq} for GHG mitigation and US\$6.2 per kg of N for ANP control (Figure 6). For GHGs, average abatement costs in 2050 for reducing CO_2, CH_4, and N_2O are US\$11, US\$22, and US\$81 per ton of CO_{2eq}, respectively (Figure S22). The most cost-effective options include improving energy production efficiency, enhancing fuel quality and efficiency, adopting clean energy sources, and afforestation. For ANPs, average MACs are US\$4 per kg of NH_3 and US\$5 per kg of NO_x in 2050, with the lowest-cost being included 4R fertilization (right type, right rate, right time, and right place), optimized livestock management, and soil/crop management (Figure S23). Several measures exhibiting negative abatement costs (indicating net cost savings), such as improving energy production efficiency, using renewable energy, and enhancing public transportation, are therefore suitable for broad adoption. Overall, agricultural practices tend to display lower unit abatement costs. However, measures such as adoption of renewable energy (within

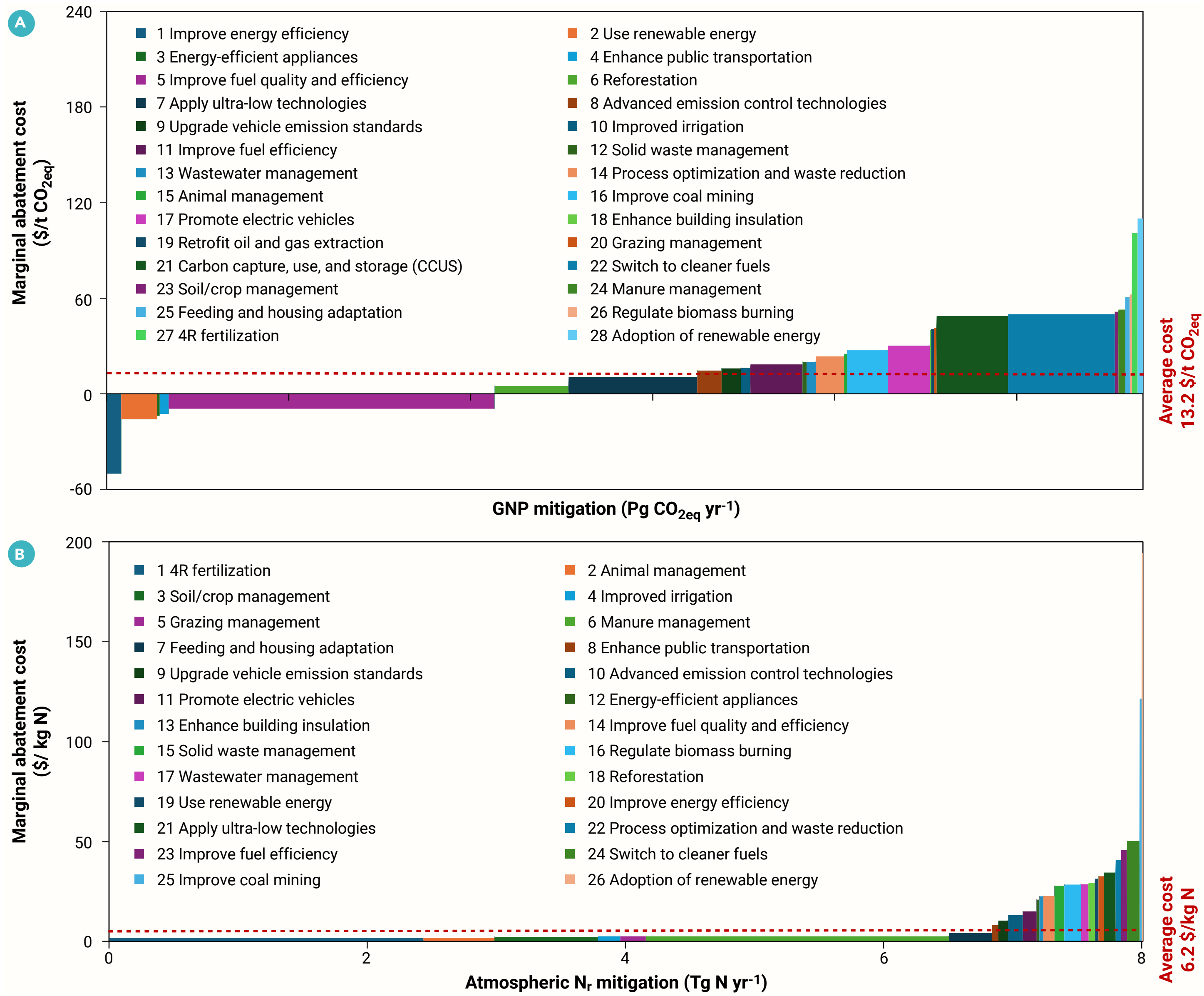

Figure 6. MACs of GHG and ANP mitigation under CCBS-high in 2050 (A) MAC of GHG mitigation, with the average cost of $13.2 per ton CO_{2eq} abated. (B) MAC of atmospheric N_r mitigation, with the average cost of $6.2 per kg N abated. The measures are ordered according to increasing MACs.

the industry sector), regulating biomass combustion, enhancing building insulation, and switching to cleaner fuels (within the industry sector) exhibit higher MACs, exceeding US$10 per kg GNP_{eq} by 2050 (Figure 5). These results suggest that, as the industrial sector encounters diminishing returns and reaches marginal cost ceilings, agricultural practices could become an increasingly cost-effective lever to boost further GHG reductions and support the carbon neutrality mandate.

Considering both mitigation efficiency and techno-economic performance, we evaluated the implementation costs and social benefits of co-control solutions with varying intensities. Across all scenarios, total social benefits from synergistic mitigation far exceed the costs, by approximately five times in 2050 (Figure 7). The CCBS-high pathway entails the largest abatement expenditures, amounting to US$200 (US$118–US$283) billion, but delivers the greatest benefits of US$959 (US$499–US$1,419) billion by 2050 (Figure 7A). Sectorally, agriculture contributes the largest share of the benefits at 38%, followed by energy (31%) and industry (16%), with households and transportation contributing 8% and 7%, respectively. Around two-thirds of total benefits arise from climate benefits, 23% from health benefits, and 15% from ecosystem benefits (Figure S24). Spatially, health co-benefits are concentrated in Hebei, Henan, Shandong, and Jiangsu, where population exposure to $PM_{2.5}$ is more severe. Ecological benefits are pronounced in southwestern and central regions, such as Hebei, Henan, Yunnan, and Sichuan, while climate-related gains are prominent in energy-exporting and consumption-intensive regions, such as Guangdong, Inner Mongolia, Shandong, and Zhejiang (Figure 8).

The CCBS-middle strategy involves roughly 70% of the implementation costs of CCBS-high, yielding net social benefits of US$774 (US$488–US$1,060) billion by 2050 (Figure 7B). In contrast, CCBS-low yields the lowest social returns, amounting to US$334 (US$241–US$428) billion by 2050, at an implementation cost of US$57 (US$43–US$70) billion, owing to its continued reliance on existing fossil fuel infrastructure and limited investment in frontier technologies. Comparing MACs in 2050, CCBS-high (US$2.8 per kg GNP_{eq}) is more cost-effective than both CCBS-middle (US$4.0 per kg GNP_{eq}) and CCBS-low (US$3.1 per kg GNP_{eq}; Figures S25 and S26). This advantage stems from the deep penetration of synergistic mitigation measures under the CCBS-high pathway, including improved fuel quality and efficiency, advanced emission control technologies, soil/crop management, and enhanced public transportation (Note S4).

Feasibility and policy implications

Our integrated multi-model framework promotes the prevailing single-pollutant, sector-isolated paradigm of environmental governance by systematically evaluating GHG and ANP emission reductions from sectoral, regional, and measure-level dimensions in China (Figures 2 and S27). The proposed GNP_{eq}

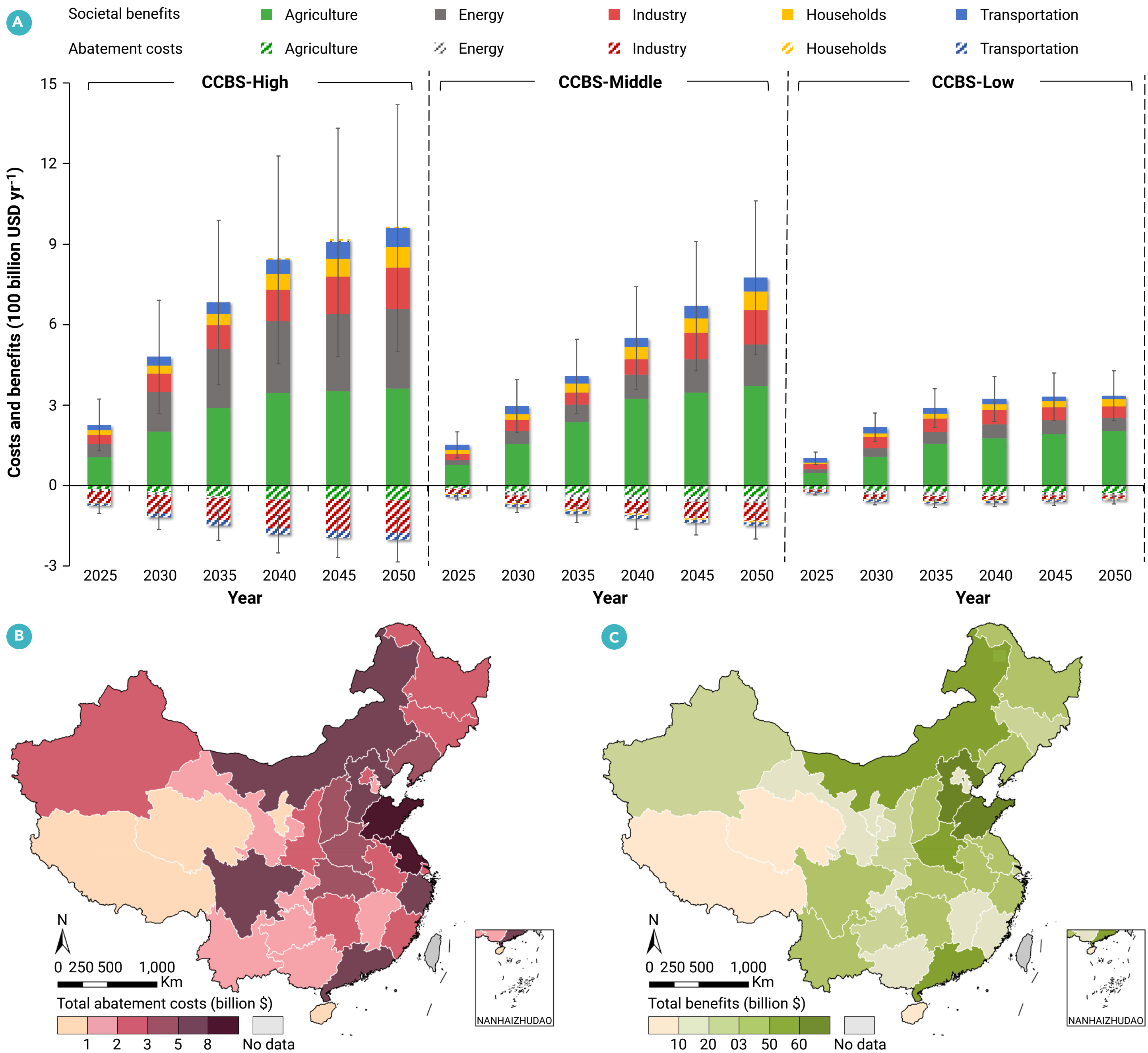

Figure 7. Cost-benefit analysis of different co-control scenarios in China (A) Total mitigation costs and benefits by sector from 2025 to 2050 (unit: US\$100 billion year^{-1}). Negative values indicate implementation costs, whereas positive values refer to societal benefits. The error bars represent the uncertainty ranges (95% confidence intervals) derived from 10,000 Monte Carlo simulations. (B and C) Spatial pattern of (B) abatement cost and (C) societal benefits in 2050 under the CCBS-high pathway.

framework bridges a critical gap in existing approaches by internalizing the societal damage costs of climate and air quality pollutants into a unified equivalency metric. This integration prevents the uncritical adoption of trade-off measures such as achieving deep CO_2 reductions at the expense of exacerbating nitrogen pollution. Crucially, the GNP_{eq} index highlights the underrecognized mitigation role of agriculture. Evaluated solely on CO_2 emissions, agriculture's contribution appears marginal compared to fossil fuel-intensive industries. However, when factoring in the disproportionate health and ecological impacts of NH_3, CH_4, and N_2O, its synergistic mitigation potential is projected to surpass that of industry by 2030, underscoring the need to prioritize high-leverage interventions along the carbon neutrality pathway.

Translating these theoretical synergies into practice requires a phased, adaptive implementation strategy that accounts for sectoral dynamics and technological readiness. Sectorally, in the near term, synergistic mitigation led by the energy and fossil fuel-based industrial sectors appears more advantageous owing to the homogeneity of CO_2 and NO_x emissions[47] and the escalating social cost of carbon.[48] In parallel, the transportation and household sectors provide immediate opportunities for synergistic abatement via electrification, clean heating, and modal shifts.[49] However, the long-term sustainability of mitigation in capital-intensive heavy industries remains contingent upon infrastructure turnover rates and the maturation of advanced technologies.[50] Key challenges include mobilizing large-scale financing for deep decarbonization and strengthening institutional capacity to manage transitions from coal-dominated systems toward emerging energy structures.[51,52] While the energy sector remains central to decarbonization, advances in hydrogen and ammonia systems may fundamentally reshape carbon-nitrogen interactions.[53] This prospect necessitates anticipatory governance to regulate potential nitrogen-related externalities through integrated regulatory standards.

As the marginal mitigation potential of heavy industry plateaus, agriculture will emerge as the critical frontier for synergistic mitigation post 2030 in China.[54,55] Unlocking this potential, however, is often hampered by the fragmented nature of rural production and the risk-averse behavior of

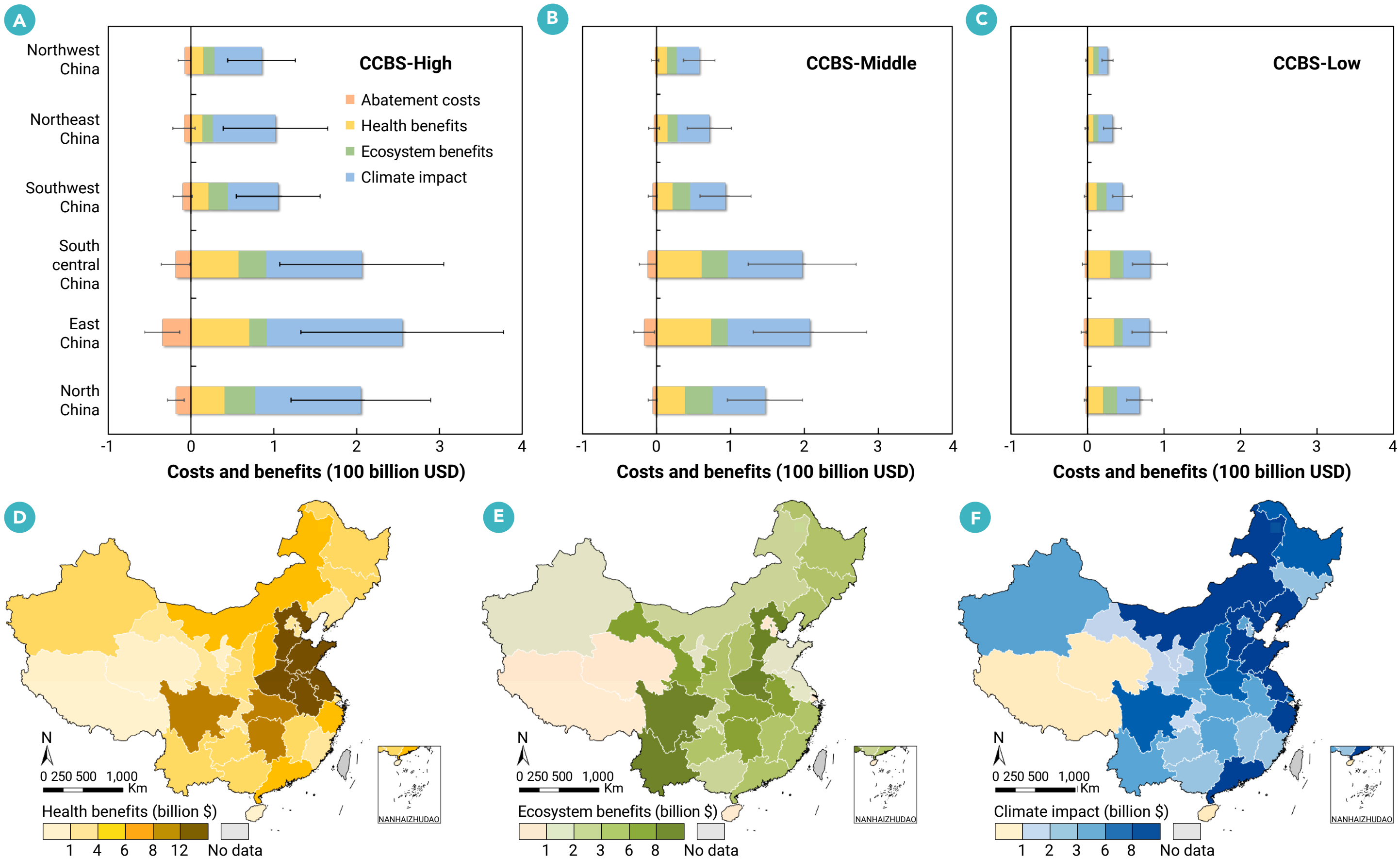

Figure 8. Societal benefits under alternative co-control scenarios in 2050 (A–C) Cost-benefit analysis across six geographic divisions in 2050 under the (A) CCBS-high, (B) CCBS-middle, and (C) CCBS-low pathways, respectively. The error bars represent the uncertainty ranges (95% confidence intervals) derived from 10,000 Monte Carlo simulations. (D–F) Spatial distribution of (D) health benefits, (E) ecosystem benefits, and (F) climate impact in 2050 under the CCBS-high pathway.

smallholders.[56] Overcoming these barriers requires moving beyond mere technological deployment to align economic incentives, enhance social acceptance, and expand local knowledge extension networks. Crucially, successful implementation is tied to the evolution of policy instruments.[44] The persistent lag in regulating agricultural nitrogen emissions (especially NH_3) remains a primary bottleneck. While incorporating NH_3 into air quality standards is a positive step, the absence of explicit reduction targets and robust enforcement limits its overall impact.[16] Establishing market-based instruments, such as tiered nitrogen credit systems or expanded emissions trading schemes that internalize both carbon and nitrogen externalities, could improve the financial viability of these measures, particularly in regions where environmental objectives face tensions with economic returns.[57,58]

Spatially, the deployment of co-control strategies should be tailored to regional socioeconomic and biogeochemical profiles.[59] For example, major urban agglomerations, such as the Beijing-Tianjin-Hebei, Yangtze River Delta, and Pearl River Delta regions, are well positioned to pioneer high-intensity, cross-sectoral mitigation measures, such as industrial upgrading and household energy transitions. Coordinated governance within these clusters facilitates infrastructure integration and policy alignment, reducing MACs while maximizing co-benefits between air quality improvement and climate objectives. In contrast, intensive agricultural hubs, such as the North China Plain and the Middle-Lower Yangtze River Basin, should prioritize low-cost, high-leverage interventions targeting non-CO_2 GHGs and nitrogen pollutants. Practices such as precision fertilization and livestock-cropland nutrient recycling could deliver massive emission reductions while simultaneously enhancing soil carbon sequestration and food security. Collectively, effective synergistic mitigation means abandoning parallel environmental agendas, instead embedding unified GHG-ANP objectives into a cohesive policy framework that balances near-term, low-regret actions with long-term structural transformation.[10]

Uncertainty and limitations

This study faces several sources of uncertainty and limitation, arising from data availability, model structure, and scenario design. First, the analytical boundary focuses on GHG and ANP, excluding nitrogen flows and impacts on aquatic systems. Emissions from certain subsectors, such as shipping and aviation within the transport sector, are not included due to data constraints. In addition, while emerging strategies, such as the use of renewable-derived ammonia as an energy carrier, have been proposed in the literature,[53] uncertainties remain regarding nitrogen leakage from alternative fuels and their future technological diffusion.[60] Further, interactions with other air pollutants (e.g., SO_2, VOCs, and primary aerosols) are not explicitly considered despite their potential influence on air quality outcomes and associated co-benefits.

Second, uncertainties are inherent in the integrated multi-model framework. Coupling CHANS, GAINS, and atmospheric modeling components requires harmonization of data across different spatial, temporal, and sectoral resolutions. This integration inevitably involves simplifications, including aggregation across regions, linearization of nonlinear processes, and approximations to maintain computational feasibility at provincial and national scales. In the air quality component, processes such as bidirectional NH_3 exchange between the surface and atmosphere remain highly uncertain and are therefore treated in a simplified manner.[61] These structural and parametric uncertainties may affect the absolute magnitude of estimated emissions, concentrations, and associated impacts.

Third, the GHG-ANP coupling index provides a policy-oriented tool for assessing co-control potential, but it is inherently normative. Weighting factors depend on assumptions regarding carbon prices and nitrogen damage valuations, which vary regionally and temporally and remain debated. Although sensitivity analyses support the robustness of the main results, GNP_{eq} should be interpreted as a comparative scoring framework rather than a physical emission metric, as it cannot fully capture spatial heterogeneity, temporal dynamics, or nonlinear damage functions. The accuracy of weighting factors could be further improved through iterative coefficient estimation systems that incorporate the physicochemical properties of pollutants and their impacts on human health and ecosystems.

Fourth, the scenario design introduces additional limitations. Each CCBS is paired with a specific SSP pathway, implying changes in socio-economic structure, demand patterns, technological progress, and policy stringency. While this approach ensures internally consistent futures, it limits the ability to isolate emission reductions attributable to underlying socio-economic changes from those due to additional co-control measures. A broader scenario matrix that varies co-control intensity while holding SSPs constant, or explores a broader range of plausible future socioeconomic trajectories, would enable a more systematic evaluation of integrated mitigation benefits. Finally, the cost-benefit analysis is subject to uncertainties in investment and operating costs, mitigation efficiencies, and long-term technological progress. Real-world feasibility also depends on factors such as policy design, institutional capacity, financing conditions, behavioral responses, and social acceptance.

To capture the propagation of uncertainties, probabilistic ranges derived from Monte Carlo simulations were incorporated to reinforce the robustness of the core findings. For instance, at the most conservative lower bound of the probabilistic estimates, the total societal benefits of synergistic mitigation consistently exceed the implementation costs (Figure 7). In addition, the strategic shift in mitigation priorities toward the agricultural sector remains statistically robust across the full uncertainty range (Figure S14). Although absolute estimates vary, the economic feasibility of co-control strategies and the policy implications remain highly robust. Future research can further reduce current uncertainties by expanding sectoral coverage, refining coupling processes, and adopting more comprehensive scenario matrices.

CONCLUSION

This study develops an integrated multi-model framework that quantitatively bridges disciplinary gaps among biogeochemical fluxes, atmospheric physicochemical feedback, and cost-benefit analysis. We demonstrate that a stringent co-control strategy could achieve reductions of 88% (80%–101%) in GHGs and 67% (50%–80%) in ANPs by 2050, generating US$959 (US$499–US$1,419) billion in net social benefits with a 5-fold return on investment. Further, by employing MACCs to evaluate cross-sectoral measures, we pinpoint cost-effective priority actions that offer actionable insights for policy optimization.

Resolving the dual crises of climate change and environmental degradation requires moving beyond fragmented governance toward dynamic co-control strategies. Our assessment reveals a critical structural turning point. As industrial mitigation approaches its marginal cost ceilings post 2030, agriculture will shift from a complementary option to the essential frontier for cost-effective synergistic mitigation. This temporary pivot in sectoral dominance necessitates a dynamic realignment of national policy priorities following the anticipated carbon peak. Methodologically, the GNP_{eq} index provides a robust framework to normalize and compare the complex social externalities of GHGs and ANPs, facilitating a systematic evaluation of cross-sectoral trade-offs. Beyond China, this study offers a scalable and transferable policy design paradigm, providing actionable quantitative evidence for rapidly developing economies that integrating deep decarbonization with sustainable nitrogen management represents an economically viable pathway to achieving multiple environmental goals.

RESOURCE AVAILABILITY

Materials availability

This study did not generate new unique materials or reagents.

Data and code availability

Data supporting the findings of this study are available within the article and its supplemental information files. Model datasets are available from the corresponding author upon reasonable request.

FUNDING AND ACKNOWLEDGMENTS

This study was supported by the National Natural Science Foundation of China (42325707 and 425B2055), the Frontiers Planet Prize (International Champion) funded by the Frontiers Research Foundation, and the Fundamental and Interdisciplinary Disciplines Breakthrough Plan of the Ministry of Education of China (JYB2025XDXM909). This research contributes to project CN 02/2022 funded by Austria's Agency for Education and Internationalization and Grant Agreement Project-101149335-SynCAN-HORIZON-MSCA-2023-PF-01 funded by the European Union. The funders had no role in study design, data collection and analysis, decision to publish, or preparation of the manuscript.

AUTHOR CONTRIBUTIONS

B.G. designed the study. X.X. prepared and analyzed the data. X.Z. provided support for modeling and impact assessment. J.X. and L.Z. performed the air quality modeling. C.W. provided support for spatial analysis. X.X., X.Z., and B.G. interpreted the results and wrote the first draft of the paper. S.Z. and W.W. revised the paper. All authors contributed to the manuscript and approved the final version.

DECLARATION OF INTERESTS

The authors declare no competing interests.

SUPPLEMENTAL INFORMATION

It can be found online at https://doi.org/10.1016/j.xinn.2026.101433.

REFERENCES

1. Galloway, J.N., Townsend, A.R., Erisman, J.W. et al. (2008). Transformation of the Nitrogen Cycle: Recent Trends, Questions, and Potential Solutions. *Science* **320**:889–892. DOI:10.1126/science.1136674
2. Heimann, M. and Reichstein, M. (2008). Terrestrial ecosystem carbon dynamics and climate feedbacks. *Nature* **451**:289–292. DOI:10.1038/nature06591
3. Deng, Z., Zhu, B., Davis, S.J. et al. (2025). Global carbon emissions and decarbonization in 2024. *Nat. Rev. Earth Environ.* **6**:231–233. DOI:10.1038/s43017-025-00658-x
4. Ministry of Ecology and Environment (2025). China's Actions for Carbon Peak and Carbon Neutrality. https://www.mee.gov.cn/ywgz/ydqhbh/qhbhlf/202511/t20251108_1132414.shtml
5. EDGAR (2024). Emissions Database for Global Atmospheric Research. EDGARv8.1. https://edgar.jrc.ec.europa.eu/index.php/dataset_ap81
6. State Council of China (2013). The Action Plan on the Prevention and Control of Air Pollution. https://www.gov.cn/zwgk/2013-09/12/content_2486773.htm
7. State Council of China (2018). Notice of the State Council on Printing and Distributing the Three-Year Action Plan for Winning the Blue-Sky Defense War. https://www.gov.cn/zhengce/content/2018-07/03/content_5303158.htm
8. Bai, Z., Winiwarter, W., Klimont, Z. et al. (2019). Further Improvement of Air Quality in China Needs Clear Ammonia Mitigation Target. *Environ. Sci. Technol.* **53**:10542–10544. DOI:10.1021/acs.est.9b04725
9. Fu, H., Zhao, K., Xie, X. et al. (2025). Contribution of Nitrogen Management to Greenhouse Gas Emission Reduction: A Case Study of China. *Environ. Sci. Technol.* **59**:9072–9081. DOI:10.1021/acs.est.4c10935
10. Yin, Z., Lei, Y., Lu, X. et al. (2025). The 2024 report of the synergetic roadmap on carbon neutrality and clean air for China: Pollution and carbon reduction promote green economic development. *Env. Sci. Ecotechnol.* **28**:100636. DOI:10.1016/j.ese.2025.100636
11. Xu, X., Zhang, X., Zou, Y. et al. (2025). Integrated carbon and nitrogen management for cost-effective environmental policies in China. *Science* **388**:1098–1103. DOI:10.1126/science.ads4105
12. Shang, F., Liu, M., Song, Y. et al. (2024). Substantial nitrogen abatement accompanying decarbonization suppresses terrestrial carbon sinks in China. *Nat. Commun.* **15**:7738. DOI:10.1038/s41467-024-52152-5
13. Li, N., Chen, W., Rafaj, P. et al. (2019). Air Quality Improvement Co-benefits of Low-Carbon Pathways toward Well Below the 2 °C Climate Target in China. *Environ. Sci. Technol.* **53**:5576–5584. DOI:10.1021/acs.est.8b06948
14. Tang, R., Zhao, J., Liu, Y. et al. (2022). Air quality and health co-benefits of China's carbon dioxide emissions peaking before 2030. *Nat. Commun.* **13**:1008. DOI:10.1038/s41467-022-28672-3
15. Zhang, Y., Smith, S.J., Bowden, J.H. et al. (2017). Co-benefits of global, domestic, and sectoral greenhouse gas mitigation for US air quality and human health in 2050. *Environ. Res. Lett.* **12**:114033. DOI:10.1088/1748-9326/aa8f76
16. Gu, B., Zhang, L., Van Dingenen, R. et al. (2021). Abating ammonia is more cost-effective than nitrogen oxides for mitigating $PM_{2.5}$ air pollution. *Science* **374**:758–762. DOI:10.1126/science.abf8623
17. Giannadaki, D., Giannakis, E., Pozzer, A. et al. (2018). Estimating health and economic benefits of reductions in air pollution from agriculture. *Sci. Total Environ.* **622–623**:1304–1316. DOI:10.1016/j.scitotenv.2017.12.064
18. Xie, Y., Wu, Y., Xie, M. et al. (2020). Health and economic benefit of China's greenhouse gas mitigation by 2050. *Environ. Res. Lett.* **15**:104042. DOI:10.1088/1748-9326/aba97b
19. Chen, Y., Shen, H., Shen, G. et al. (2024). Substantial differences in source contributions to carbon emissions and health damage necessitate balanced synergistic control plans in China. *Nat. Commun.* **15**:5880. DOI:10.1038/s41467-024-50327-8
20. Gu, B., Ju, X., Chang, J. et al. (2015). Integrated reactive nitrogen budgets and future trends in China. *Proc. Natl. Acad. Sci. USA* **112**:8792–8797. DOI:10.1073/pnas.1510211112
21. Wang, S., Zhang, X., Wang, C. et al. (2020). A high-resolution map of reactive nitrogen inputs to China. *Sci. Data* **7**:379. DOI:10.1038/s41597-020-00718-5

22. MEIC (2023). Multi-resolution Emission Inventory model for Climate and air pollution research (MEIC v1.4). http://meicmodel.org.cn/
23. Duan, J., Liu, H., Zhang, X. et al. (2024). Agricultural management practices in China enhance nitrogen sustainability and benefit human health. *Nat. Food* **5**:378–389. DOI:10.1038/s43016-024-00953-8
24. Zhang, X., Gu, B., van Grinsven, H. et al. (2020). Societal benefits of halving agricultural ammonia emissions in China far exceed the abatement costs. *Nat. Commun.* **11**:4357. DOI:10.1038/s41467-020-18196-z
25. Zhang, X., Sun, Y., Gao, Y. et al. (2026). Halving global ammonia emissions with cost-effective measures. *Nat. Sustain.* **9**:247–259. DOI:10.1038/s41893-025-01723-5
26. Zhang, Q.Y., Cai, B.F., Wang, M.D. et al. (2022). City level CO_2 and local air pollutants co-control performance evaluation: A case study of 113 key environmental protection cities in China. *Adv. Clim. Chang. Res.* **13**:118–130. DOI:10.1016/j.accre.2021.10.002
27. Wang, Y., Ni, J., Xu, K. et al. (2024). Intricate synergistic effects between air pollution and carbon emission: An emerging evidence from China. *Environ. Pollut.* **349**:123851. DOI:10.1016/j.envpol.2024.123851
28. Klimont, Z. and Winiwarter, W. (2011). Integrated Ammonia Abatement - Modelling of Emission Control Potentials and Costs in GAINS (IIASA). https://pure.iiasa.ac.at/9809
29. GBD (2021). Global Burden of Disease Study 2021 (GBD 2021) Data Resources. https://ghdx.healthdata.org/gbd-2021
30. Brink, C., van Grinsven, H., Jacobsen, B.H. et al. (2011). In Costs and Benefits of Nitrogen in the Environment, M.A. Sutton, C.M. Howard, and J.W. Erisman et al., eds. (Cambridge University Press), pp. 513–540. DOI:10.1017/CBO9780511976988.025
31. Yang, P., Yao, Y.F., Mi, Z. et al. (2018). Social cost of carbon under shared socioeconomic pathways. *Glob. Environ. Change* **53**:225–232. DOI:10.1016/j.gloenvcha.2018.10.001
32. Gong, C., Tian, H., Liao, H. et al. (2024). Global net climate effects of anthropogenic reactive nitrogen. *Nature* **632**:557–563. DOI:10.1038/s41586-024-07714-4
33. Gu, B., Zhang, X., Lam, S.K. et al. (2023). Cost-effective mitigation of nitrogen pollution from global croplands. *Nature* **613**:77–84. DOI:10.1038/s41586-022-05481-8
34. Zhang, X., Wu, Y., Liu, X. et al. (2017). Ammonia Emissions May Be Substantially Underestimated in China. *Environ. Sci. Technol.* **51**:12089–12096. DOI:10.1021/acs.est.7b02171
35. Guan, Y., Shan, Y., Huang, Q. et al. (2021). Assessment to China's Recent Emission Pattern Shifts. *Earth Future* **9**:e2021EF002241. DOI:10.1029/2021EF002241
36. Zheng, B., Tong, D., Li, M. et al. (2018). Trends in China's anthropogenic emissions since 2010 as the consequence of clean air actions. *Atmos. Chem. Phys.* **18**:14095–14111. DOI:10.5194/acp-18-14095-2018
37. Ministry of Agricultural and Rural Affairs (2015). The Zero Increase of Fertilizer and Pesticides Action. https://www.moa.gov.cn/govpublic/ZZYGLS/201505/t20150525_4614695.htm
38. Chen, J., Gao, M., Cheng, S. et al. (2020). County-level CO_2 emissions and sequestration in China during 1997–2017. *Sci. Data* **7**:391. DOI:10.1038/s41597-020-00736-3
39. Jiang, L., Chen, Y., Zhou, H. et al. (2020). NO_x emissions in China: Temporal variations, spatial patterns and reduction potentials. *Atmos. Pollut. Res.* **11**:1473–1480. DOI:10.1016/j.apr.2020.06.003
40. Wang, C., Liu, Z., Zhang, X. et al. (2025). Managing Ammonia for Multiple Benefits Based on Verified High-Resolution Emission Inventory in China. *Environ. Sci. Technol.* **59**:5131–5144. DOI:10.1021/acs.est.4c12558
41. Cui, X., Shang, Z., Xia, L. et al. (2022). Deceleration of Cropland-N_2O Emissions in China and Future Mitigation Potentials. *Environ. Sci. Technol.* **56**:4665–4675. DOI:10.1021/acs.est.1c07276
42. Gidden, M.J., Riahi, K., Smith, S.J. et al. (2019). Global emissions pathways under different socioeconomic scenarios for use in CMIP6: a dataset of harmonized emissions trajectories through the end of the century. *Geosci. Model Dev.* **12**:1443–1475. DOI:10.5194/gmd-12-1443-2019
43. Dong, J., Cai, B., Zhang, S. et al. (2023). Closing the Gap between Carbon Neutrality Targets and Action: Technology Solutions for China's Key Energy-Intensive Sectors. *Environ. Sci. Technol.* **57**:4396–4405. DOI:10.1021/acs.est.2c08171
44. Wu, Y., Xi, X., Tang, X. et al. (2018). Policy distortions, farm size, and the overuse of agricultural chemicals in China. *Proc. Natl. Acad. Sci. USA* **115**:7010–7015. DOI:10.1073/pnas.1806645115
45. Xie, Y., Wu, Y., Zhao, M. et al. (2025). Accelerated attainment of global air quality standards with disproportional health co-benefits under the 1.5 °C target. *Nat. Commun.* **17**:579. DOI:10.1038/s41467-025-67276-5
46. Xia, L., Lam, S.K., Chen, D. et al. (2017). Can knowledge-based N management produce more staple grain with lower greenhouse gas emission and reactive nitrogen pollution? A meta-analysis. *Glob. Chang. Biol.* **23**:1917–1925. DOI:10.1111/gcb.13455
47. Shi, Q., Zheng, B., Zheng, Y. et al. (2022). Co-benefits of CO_2 emission reduction from China's clean air actions between 2013-2020. *Nat. Commun.* **13**:5061. DOI:10.1038/s41467-022-32656-8
48. Liu, A., Chen, Y. and Cheng, X. (2022). Social cost of carbon under a carbon-neutral pathway. *Environ. Res. Lett.* **17**:054031. DOI:10.1088/1748-9326/ac6819
49. Wei, H., Yu, Q., Chen, D. et al. (2024). Residential energy transition and chronic respiratory diseases. *Innovation* **5**:100597. DOI:10.1016/j.xinn.2024.100597
50. Wang, F., Harindintwali, J.D., Yuan, Z. et al. (2021). Technologies and perspectives for achieving carbon neutrality. *Innovation-Amsterdam* **2**:100180. DOI:10.1016/j.xinn.2021.100180
51. Zhao, H., Kamp, L.M. and Lukszo, Z. (2022). The potential of green ammonia production to reduce renewable power curtailment and encourage the energy transition in China. *Int. J. Hydrogen Energy* **47**:18935–18954. DOI:10.1016/j.ijhydene.2022.04.088
52. Yang, G., Zha, D., Cao, D. et al. (2024). Time for a change: Rethinking the global renewable energy transition from the Sustainable Development Goals and the Paris Climate Agreement. *Innovation* **5**:100582. DOI:10.1016/j.xinn.2024.100582
53. Zhang, X., Sabo, R., Rosa, L. et al. (2024). Nitrogen management during decarbonization. *Nat. Rev. Earth Environ.* **5**:717–731. DOI:10.1038/s43017-024-00586-2
54. Gao, Y., Wang, S., Chen, L. et al. (2024). Achieving accurate regional carbon-sink accounting and its significance for "missing" carbon sinks. *Innovation* **5**:100552. DOI:10.1016/j.xinn.2023.100552
55. Wang, L., Garland, G.M., Ge, T. et al. (2025). Integrated strategies for enhancing agrifood productivity, lowering greenhouse gas emissions, and improving soil health. *Innovation* **6**:101006. DOI:10.1016/j.xinn.2025.101006
56. Cui, Z., Zhang, H., Chen, X. et al. (2018). Pursuing sustainable productivity with millions of smallholder farmers. *Nature* **555**:363–366. DOI:10.1038/nature25785
57. Li, W. and Jia, Z. (2017). Carbon tax, emission trading, or the mixed policy: which is the most effective strategy for climate change mitigation in China? *Mitig. Adapt. Strateg. Glob. Chang.* **22**:973–992. DOI:10.1007/s11027-016-9710-3
58. Gu, B., van Grinsven, H.J.M., Lam, S.K. et al. (2021). A Credit System to Solve Agricultural Nitrogen Pollution. *Innovation* **2**:100079. DOI:10.1016/j.xinn.2021.100079
59. Yu, B., Zhao, Z., Wei, Y.M. et al. (2023). Approaching national climate targets in China considering the challenge of regional inequality. *Nat. Commun.* **14**:8342. DOI:10.1038/s41467-023-44122-0
60. Wolfram, P., Kyle, P., Zhang, X. et al. (2022). Using ammonia as a shipping fuel could disturb the nitrogen cycle. *Nat. Energy* **7**:1112–1114. DOI:10.1038/s41560-022-01124-4
61. Zhu, L., Henze, D., Bash, J. et al. (2015). Global evaluation of ammonia bidirectional exchange and livestock diurnal variation schemes. *Atmos. Chem. Phys.* **15**:12823–12843. DOI:10.5194/acp-15-12823-2015